SPE-202030-MS

From Qualitative Interpretation to Quantitative Analysis: Prediction of Properties of Geological Bodies by Using the Spectral Decomposition Attribute – Case Study of Achimov Turbidity System in West-Siberia

Roman Petrovich Volkov, Dmitrii Sergeyevich Volkov, and Georgii Sergeyevich Kozhevnikov, Laboratory of Geology and Sedimentary Basins Modeling, LLC

This paper was prepared for presentation at the SPE Russian Petroleum Technology Conference originally scheduled to be held in Moscow, Russia, 12-14 October 2020. Due to COVID-19 the physical event was postponed until 26 – 29 October 2020 and was changed to a virtual event. The official proceedings were published online on 26 October 2020.

Abstract

The spectral decomposition attribute map is one of the most representative data for geological and qualitative geophysical interpretation. The specified technique using RGB mixing allows you to confidently map the seismic recording anomalies that do not appear when analyzing the full spectrum of the signal, as well as evaluate the amplitude response for the center frequency of the analyzed range. However, the question arises the applicability of the results of spectral decomposition in the process of quantitative seismic data interpretation.

There are a number of works, such as Widess (1973), J. Gridley and G. Partyka (1997), Butorin A.V. (2016), which indicate the possibility of using the spectral decomposition results when performing a quantitative assessment of the allocated geological objects thicknesses. This task is relevant because it allows you to add additional information extracted from the amplitudes of a limited frequency range at the stage of dynamic interpretation. Along with, an additional advantage of this technique is the possibility of an independent rapid assessment of the quantitative parameters of geological objects.

In this article, we propose an approach for predicting net thickness using spectral decomposition attribute and apply it to the Achimov wedge-shaped complex. These deposits are characterised by a complex distribution of sands and the occurrence of thin-bed sand bodies that are below the seismic resolution limit.

Introduction

In the late 90s of the XX century, the technology of spectral decomposition arose, which allows analysing the amplitude characteristics of the wavefield in terms of frequency components. Currently, many articles and scientific papers on spectral analysis of the wave field and aspects of its practical application have been published. However, in most production reports, this attribute is used in the process of geological and geophysical interpretation of the 3D seismic data only at a qualitative level - the visibility and representativeness of the analyzed maps allow outline to confidently geological objects. That either does not appear at all or manifest themselves significantly worse when analyzing standard attributes, calculated from data of the full frequency range.

In this case, questions arise Should we consider the results of calculating the spectral decomposition attribute only in the form of a certain amplitude frequency characteristic of the studied section, which has qualitative connections with the geomorphological features of the analyzed stratigraphic surface? Is it allowed the possibility of quantitative calculations of interpreted geological objects, characterized by increased filtration and capacitive properties?

So, in the works of Widess (1973), J. Gridley and G. Partyka (1997), Butorin A.V. (2016) discusses prospects and proposes methods for the spectral decomposition attribute maps quantitative interpretation. In general, they are united by a common approach the prediction of promising geological objects thicknesses, based on the study of the interference interaction of a plane wave from the top and the bottom of a thin acoustic contrast layer.

The aim of this work is the practical implementation of the proposed approach on the quantitative prediction of the net reservoir thickness using the analysis of the wavefield, characterizing as a "thin" layer.

In this article, theoretical aspects of time frequency transformations are described, wavefield modeling is performed, a solution of the inverse problem for model data is presented, which is transferred to real data 3D seismic data one of the fields in Western Siberia with deposits in the Achimov clinoform complex. In addition, a qualitative geological interpretation of the results of spectral decomposition with the involvement of paleogeomorphological analysis is presented, as well as a comparison of the predicted thickness of the Achimov sandstone using the proposed method with the traditional approach based on inversion transformations.

Theory

There are many difficulties for seismic data interpreters in the process of studying thin geological objects and layers. One of these is the presence of effects of constructive and destructive interference with varying layer thickness. So, constructive interference (tuning effect) occurs when the signal from the top and the bottom of a thin layer is summed in phase, the thickness of which is ¼ of the wavelength of the dominant signal period. In the seismic section, it is possible to distinguish between reflections from the boundaries of the formations whose thickness values in most cases exceed ¼ of the wavelength, while a thin layer appears only in the form of a change in amplitudes. (Saadatinejad et al., 2011) A legitimate question arises: what is considered a "thin" layer and at what seismic scale of research?

The application of the spectral decomposition technique, in this case allows us to estimate the thicknesses of studied objects at a qualitative level. Partyka (1999) provides a classic example of using this attribute to determine the relative thickness of riverbed deposits. It has been established that the "thin" sections of the channel are best recorded on the spectral decomposition amplitude maps in the high frequency range, while the increased thickness of the channel deposits is most clearly reflected in the low frequency range. Laughlin et al. (2002) provided a pictorial diagram of this case. In the marginal sections of the channel, where the sediment thickness is not large, the tuning effect is observed on the spectral component of high frequencies. In the center of the channel, where thickness reaches its maximum values, the tuning effect is fixed on the spectral component of low frequencies (Figure 1).

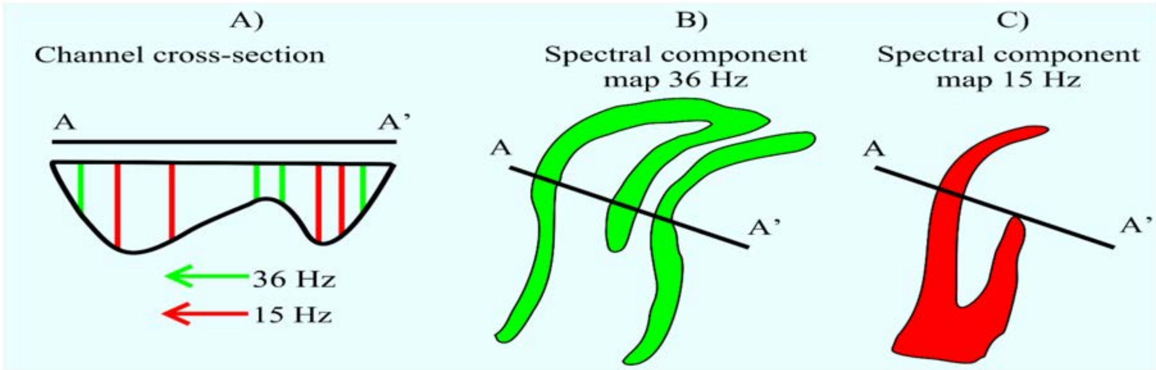

Figure 1.—A diagram showing the relationship between the tuning effect and the spectral components amplitude on the example of the channel model: a) section through the channel mode, b) a high frequencies spectral component map (36 Hz), c) a low frequencies spectral component map (15 Hz)

Besides, amplitude maps involved in the analysis of the spectral components also have differences among themselves, which are explained by the difference in the mathematical apparatus when implementing the calculation of the spectral decomposition attribute. We present two of the most used approaches - fast Fourier transform (FFT) and continuous wavelet transform (CWT).

Fast Fourier Transform

Seismic data Fourier transform F(ω) in the time domain f(t) has the following mathematical representation :

$$F(\omega) = \int_{-\infty}^{+\infty} f(t) e^{-i\omega t} dt$$

Where t time. Using Fourier transform, a nonstationary signal demonstrates general frequency distribution of the signal, when transitioning to the frequency domain.

However, this transform is not suitable for seismic data analysis, because frequency composition changes over time.

Analysis of the seismic data considered stationary in a small window, and then the Fourier transform of each segment, displays the frequency composition of the signal in this period. (Chakraborty and Okaya, 1995; Zabihi and Siahkoohi, 2006). It is possible to extract the frequency content of the signal and get a two-dimensional representation of the frequency time relationship when the time window in question correctly shifted. This two-dimensional representation is known as the Short Time Fourier Transform. The fast Fourier transform based on this technique. Short Time Fourier Transform S (ω,τ) is expressed mathematically by the internal product of the signal f(t) with the time shifted window function φ(t):

$$F(\omega) = \int_{-\infty}^{+\infty} f(t) \overline{\varphi}(t-\tau) e^{-i\omega t} dt$$

Where window function φ (t) centered at given time t = τ, τ – shift parameteshigts r,$\overline{\varphi}$ complex conjugate functions φ.

Continuous Wavelet Transform (CWT)

Continuous Wavelet Transform, introduced by Morlet et al. (1982), is another method for the signal frequency components analysis. As opposed to the Fourier transform, CWT uses a variable window length. The time resolution decreases, and the frequency resolution increases, if the length of the interval, in which the window function is different from zero, increases. On the other hand, the time resolution increases, and the frequency resolution decreases, when the interval length decreases. (Mallet, 1999).

Continuous Wavelet Transform consists of wavelets that are functions defined as ψ (t) $\epsilon L^2(R)$, that have a zero mean value, which localized in both time and frequency (Sinha et al., 2005). Each wavelet's basis is generated by extending and transforming a two-parameter function known as the mother wavelet ψ (t). We can represent all functions in the basis using transformations and scaling of the mother wavelet, taking into account a wavelet's basis

$$\psi_{\sigma,\tau}(t) = \frac{1}{\sqrt{\sigma}}\,\psi\left(\frac{t-\tau}{\sigma}\right)$$

Where $\tau \epsilon R$, $\sigma \neq 0$, σ and τ transformation and scaling parameters.

This formula shows the wavelet shrinks, its spectrum expands, and the maximum frequency shifts to a higher value when the value of σ increases. Conversely, the value of σ decreases, its spectrum shrinks, and the maximum frequency shifts to a lower value, when a wavelet scaled so that it expands (Chopra and Marfurt, 2015). Continuous wavelet transform defined as the inner product of the wavelet family$\psi_{\sigma,\tau}$ (t) with a signal f (t):

$$Fw(\sigma, \tau) = \int_{-\infty}^{+\infty} f(t)\frac{1}{\sqrt{\sigma}}\,\overline{\psi}\left(\frac{t-\tau}{\sigma}\right)dt$$

Where $\overline{\psi}$-complex conjugate ψ, F_W (σ,τ)-time scale map.

The kernel of the wavelet operator is scaled with a coefficient of $\frac{1}{\sigma}$ and transformed with parameter τ to obtain the wavelet coefficients F_W (σ,τ), at each scale (i.e. for each value σ). For performing spectral decomposition using the CWT, the following wavelets usually used: Morlet, Gaussian and Mexican Hat

Theoretical assessment of the modeling

Let's proceed to the spectral decomposition possibilities theoretical assessment by means of modeling. In this case, it is preparation for the solution of the inverse problem, a source of hypothesis testing and information content of the proposed method. Performing this task, it is quite informative to consider the acoustically contrasting wedge model, in which thickness changes within the required values for research. We synthesize these models, the maximum time thickness of which is 30 ms, by performing convolution with Ricker, Ormsby, and Gauss wavelets at equal values of the central frequency and their duration. We will analyze the amplitude response, the wavefield, and the possibility of restoring thickness using theoretical wavelets, for the obtained results.

The Riker wavelet is a zero phase signal with a central peak and two smaller side lobes (Figure 2 - Figure 4 (A)). Mathematically, it can be set by only one parameter – the central frequency f (H.Ryan., 1994):

$$A_{Ricker}(t) = (1 - 2\pi^2 f^2 t^2)e^{-\pi^2 f^2 t^2}$$

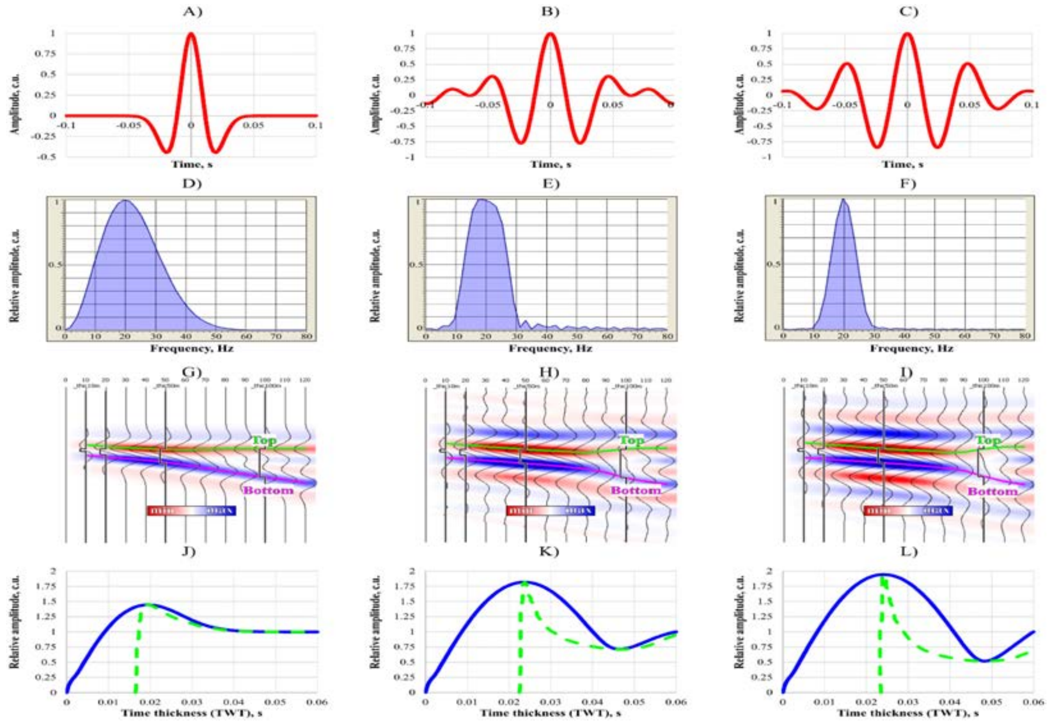

Figure 2.—The application of wavelets: A) Ricker B) Ormsby C) Gauss with a central frequency of 20 Hz to perform theoretical modeling. The amplitude-frequency characteristics of the analyzed wavelets are presented: D) Ricker E) Ormsby F) Gauss; synthesized wedge models using wavelets: G) Ricker H) Ormsby I) Gauss; amplitude response (expressed in relative values) from the top of a synthetic wedge model obtained by convolution with a signal J) Ricker K) Ormsby L) Gauss

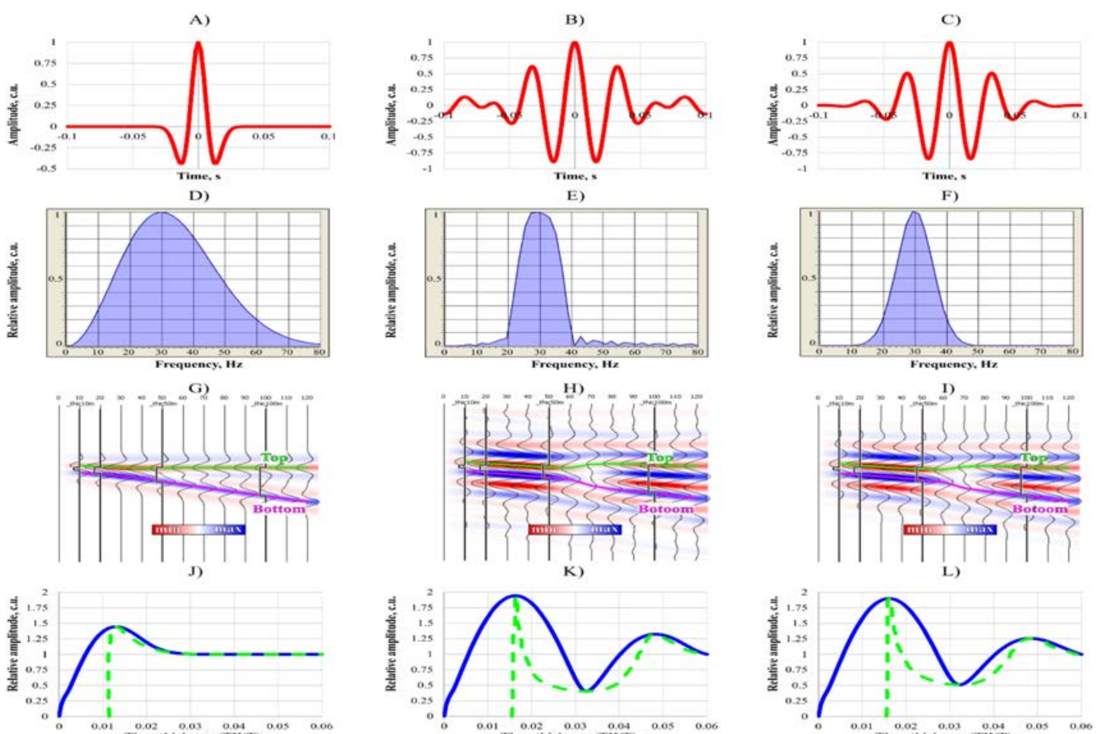

Figure 3.—The application of wavelets: A) Ricker B) Ormsby C) Gauss with a central frequency of 30 Hz to perform theoretical modeling. The amplitude-frequency characteristics of the analyzed wavelets are presented: D) Ricker E) Ormsby F) Gauss; synthesized wedge models using wavelets: G) Ricker H) Ormsby I) Gauss; amplitude response (expressed in relative values) from the top of a synthetic wedge model obtained by convolution with a signal J) Ricker K) Ormsby L) Gauss

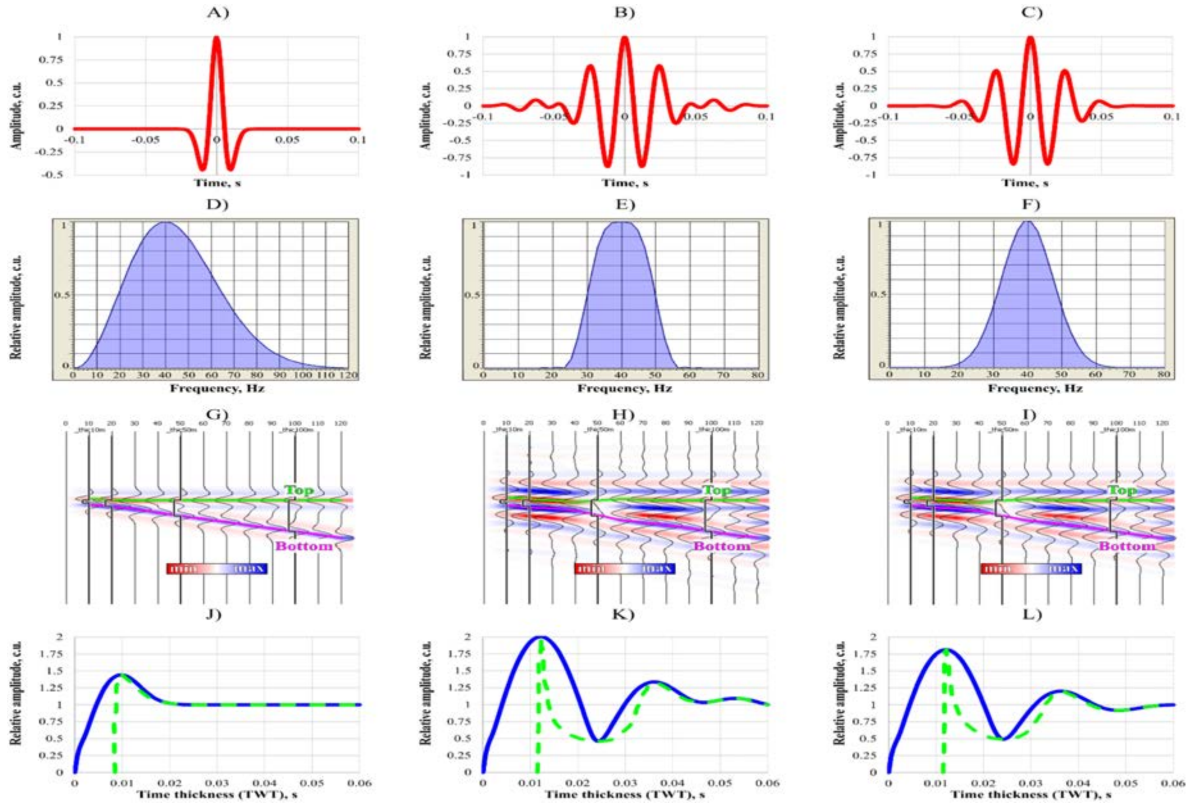

Figure 4—The application of wavelets: A) Ricker B) Ormsby C) Gauss with a central frequency of 40 Hz to perform theoretical modeling. The amplitude-frequency characteristics of the analyzed wavelets are presented: D) Ricker E) Ormsby F) Gauss; synthesized wedge models using wavelets: G) Ricker H) Ormsby I) Gauss; amplitude response (expressed in relative values) from the top of a synthetic wedge model obtained by convolution with a signal J) Ricker K) Ormsby L) Gauss

The Riker wavelet spectrum estimation demonstrates a wide frequency range, which further influences the response behavior of amplitudes in the wedge seismic model. The calculated model wavefield analysis (Figure 2 - Figure 4 (G)) is quite simple. The amplitude peak value reliably reflects the boundaries of the wedge at a thickness greater than ¼ of the signal period. This is an advantage of this model. However, there is a difference in the size of the seismic resolution threshold. According to the theoretical estimate, the resolution limit for the Riker wavelet with a central frequency of 30 Hz is about 8.3 ms, while according to the simulation results, the tuning effect observed at layer thickness 6.5 ms (Figure 2 - Figure 4 (J)).

The Ormsby wavelet is also zero phase and defined by a trapezoid shape (the boundaries of the trapezium-frequency f_1-f_4) in the frequency spectrum. Mathematically, the equation is expressed as follows (H.Ryan., 1994):

$$A_{Ormsby}(t) = \frac{\pi}{f_4 - f_3}[f_4^2 sinc^2(\pi f_4 t) - f_3^2 sinc^2(\pi f_3 t)] - \frac{\pi}{f_2 - f_1}[f_2^2 sinc^2(\pi f_2 t) - f_1^2 sinc^2(\pi f_1 t)]$$

This signal has many side lobes, which later complicates the analyzed wavefield during modeling. There are many interference minima and maxima, which complicate the correlation and do not allow us trace the position of the wedge boundaries confidently, when considering the seismic wedge model synthesized using the Ormsby wavelet. However, at the points where constructive and destructive interference observed, the peak value of the amplitude confidently reflects the desired boundary. Peak values of the amplitude at large wedge thickness more reliably describe the position of the boundary, when the Central frequency of the signal increases. The theoretical estimate of resolution limit for the Ormsby wavelet with a central frequency of 30 Hz is about 8.3 ms, according to the simulation results 8.25 ms. This fact is one of the advantages of using this wavelet because model thickness, equal to a quarter of the period, corresponds to the tuning effect.

The Gauss wavelet has mostly similar characteristics to the Ormsby wavelet described above. The signal defined as a cosine function damped by a Gauss function with a width proportional to the width of the spectrum (Figure 2 - Figure 4 (E)) at a value of 60% of the amplitude level. The imwavelet has the following mathematical representation (K. Wawrzyniak., 2009):

$$A_{Gaussian}(t) = e^{-\left(\frac{t}{a}\right)^2} \cos(2\pi f t)$$

This signal differs from others by having fewer side lobes in the time domain, as well as a Gaussian distribution of the envelope amplitude and the amplitude-frequency spectrum (Figure 2 - Figure 4 (F)). Referring to the description of the model synthesized using the Gauss wavelet (Figure 2 - Figure 4 (I)), we can also notice similarities with the above described seismic wedge model for the Ormsby wavelet (Figure 2 - Figure 4 (L)).

Therefore, based on the formulation of the modeling problem, it is possible to select and use the probing wavelet to build the model. In this case, and in the future, the main task of modeling is to study the connections between the wedge top amplitude response and the model thickness at values that do not exceed the threshold for the resolution of the signal. In the seismic model building process, it is appropriate to use both Ormsby and Gauss wavelets and the Riker wavelet with subsequent bandpass filtering of the model or further spectral decomposition. In addition, we can use the approach of building synthetic wedge models using extracted wavelets from the spectral decomposition cubes of 3D seismic data, which will be discussed later.

Modeling

Modeling using the received wavelets from the spectral components of 3D seismic data has a practical interest in this work. Cubic spectral decomposition coefficient is the calculation result. Additionally, the selection of the optimal spectrum bandwidth adjusted.

So, if the analysis assumes the use of high-frequency components of the spectrum, it is recommended to select the frequency band based on the octave scale (Figure 5) which divides them so that each subsequent interval exceeds the previous one by an octave. This technique used to eliminate the Gibbs effect, which can cause a lot of reverberation in the wavefield, the amplitude and number of which is proportional to the steepness of the frequency slice. This effect most often seen with a narrow bandwidth at high frequencies.

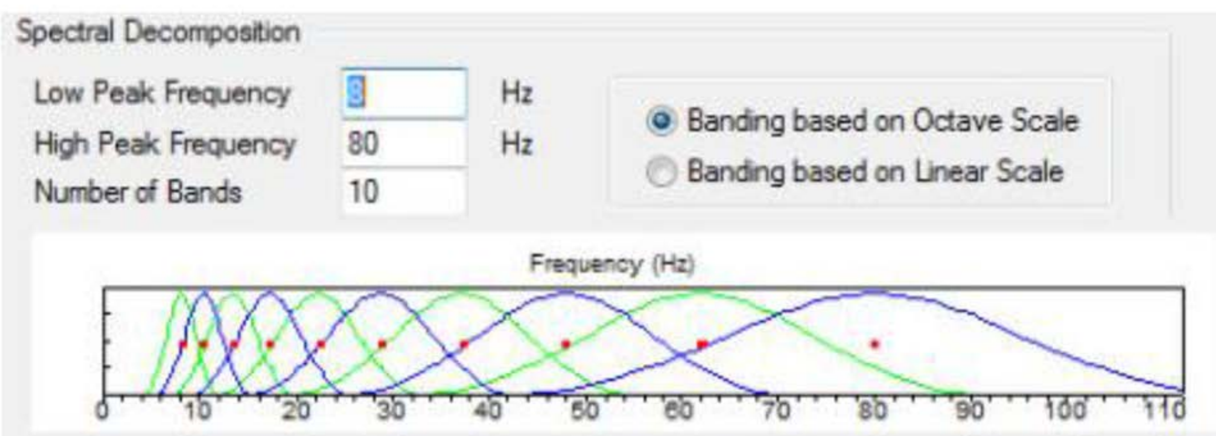

Figure 5.—Spectral decomposition attribute calculation with the choice of bandwidth based on the octave scale

To compare the methods for calculating the spectral decomposition attribute, the wavelets in the range of the Achimov clinoform complex are estimated using the example of high frequency cubes (40 Hz) with a bandwidth selection based on a linear (Model A Figure 6 (A)) and octave (model B Figure 6 (B)) scale.

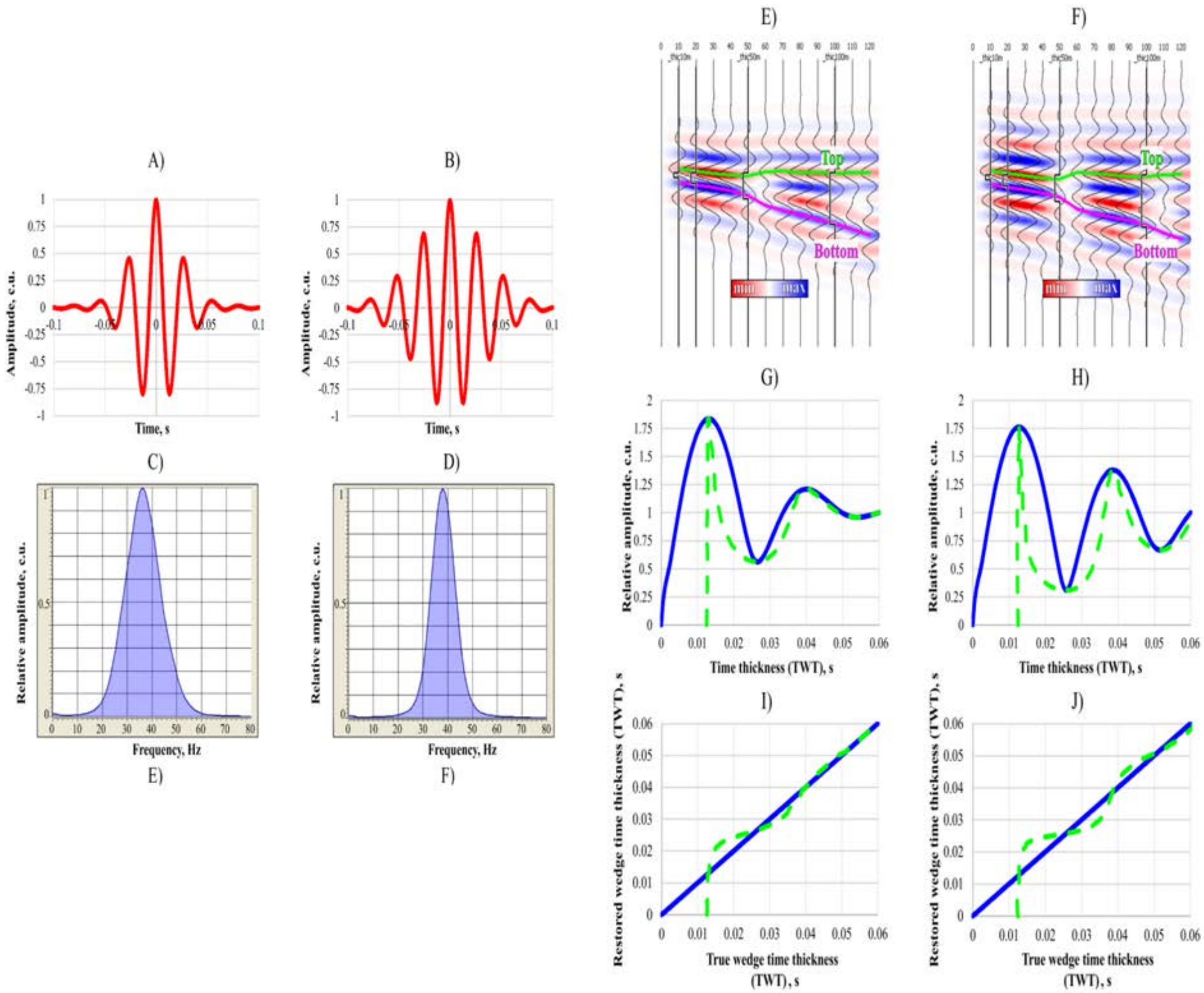

Figure 6.—Comparison of the extracted wavelets over the cube of the spectral decomposition: A) 41 Hz with the choice of the frequency bandwidth based on the octave scale (hereinafter 41 Hz) and B) 40 Hz with the choice of the frequency bandwidth based on the linear scale (further 40 Hz). Presented: amplitude-frequency characteristics for the received wavelets according to the cube of spectral decomposition: B) 41 Hz D) 40 Hz; synthesized wedge models using these wavelets: E) 41 Hz E) 40 Hz; amplitude response (expressed in relative values) from the top of the wedge synthetic model obtained by convolution with the signal: G) 41 Hz H) 40 Hz; the deviation of the time thickness restored values on the isochron map from the true values for the convolutional model of the wedge by the signal: I) 41 Hz K) 40 Hz

The differences between synthesized models of an acoustically contrasting seismic wedge for two cases of estimated wavelets, as well as the amplitude response from wedge top, expressed in relative values, clearly shown. Therefore, when considering model A (Figure 6 (D)), a complex interference pattern observed. The response of amplitudes from top and bottom of the layer has several high amplitude minima and maxima. In addition, correlation of wedge boundaries in this model does not exactly correspond to their actual position. The maximum constructive interference achieved when the time model thickness is 6.25 ms, which coincides with theoretical calculations (Figure 6 (G, I)).

For model B (Figure 6 (F)), the wavefield characterized as weakly interferential. The response of amplitudes from top and bottom of the layer has a single high-amplitude maximum. The correlation of the wedge boundaries by the peak value of amplitudes in this model corresponds more precisely to their real position. The maximum constructive interference achieved when the time model thickness is 6.1 ms, which is close enough to the theoretical value (Figure 6 (H, J)).

Further analysis consists in wavelets estimation in the Achimov clinoform interval by spectral components with their further use in the construction of acoustically contrasting synthetic wedge models. In the spectral characteristic of the studied section interval, we will select the low-medium and high frequency ranges, in each of which we will select analyzed frequency value (Figure 7). These frequencies allow us to study acoustically contrasting geological features of the section structure at various seismic scales. Large objects are most accurately interpreted in the low-frequency zone. With a thickness decrease of the desired geological bodies or their structural elements, it is necessary to proceed to the analysis of higher-frequency components of the spectrum. According to this principle, spectral decomposition cubes attributes with a central frequency of 19.4 Hz (20 Hz can be assumed), 31 Hz (30 Hz can be assumed), and 41 Hz (40 Hz can be assumed) were selected. The choice of these frequencies is based on the statement above, as well as on the representativeness of the spectral decomposition attribute map using RGB blending.

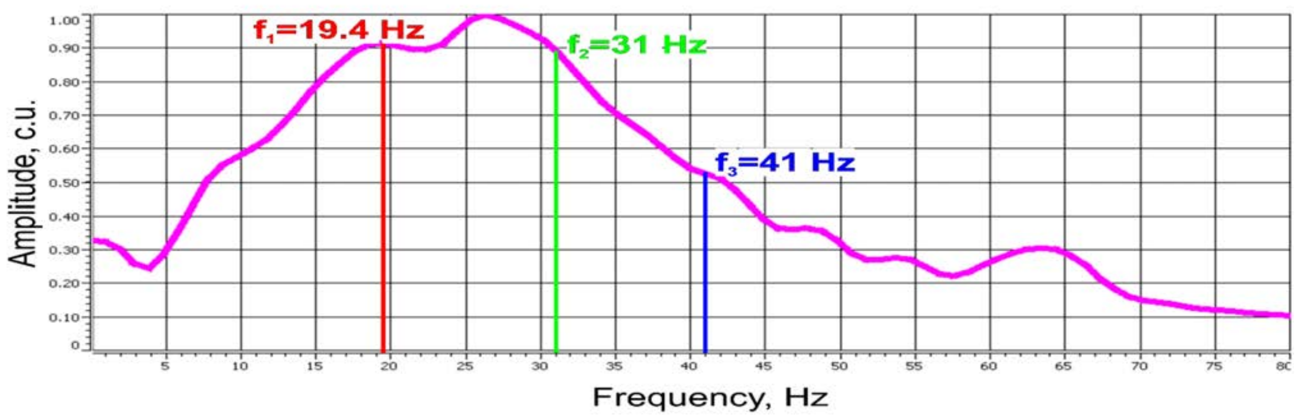

Figure 7—The amplitude spectrum calculated in the interval of the Achimov clinoform complex. For further research, the spectral decomposition attribute cubes with a central frequency of 19.4 Hz (conventionally possible to accept 20 Hz), 31 Hz (conventionally possible to accept 30 Hz), 41 Hz (conventionally possible to accept 40 Hz) were selected.

We determine the quantitative parameters of the acoustically contrasting wedge model used to obtain synthetic time sections. Acoustic impedance for this model was set solely by changing the values of p-wave velocity, which were estimated, based on the well logging interpretation results. Therefore, interval velocities in clays are taken equal to 4500 m/s, sandstones – 4200 m/s. The maximum wedge thickness is about 120 m (Figure 8). Based on the presented model, synthetic sections obtained as a result of convolution with extracted wavelets for three central frequencies are demonstrated.

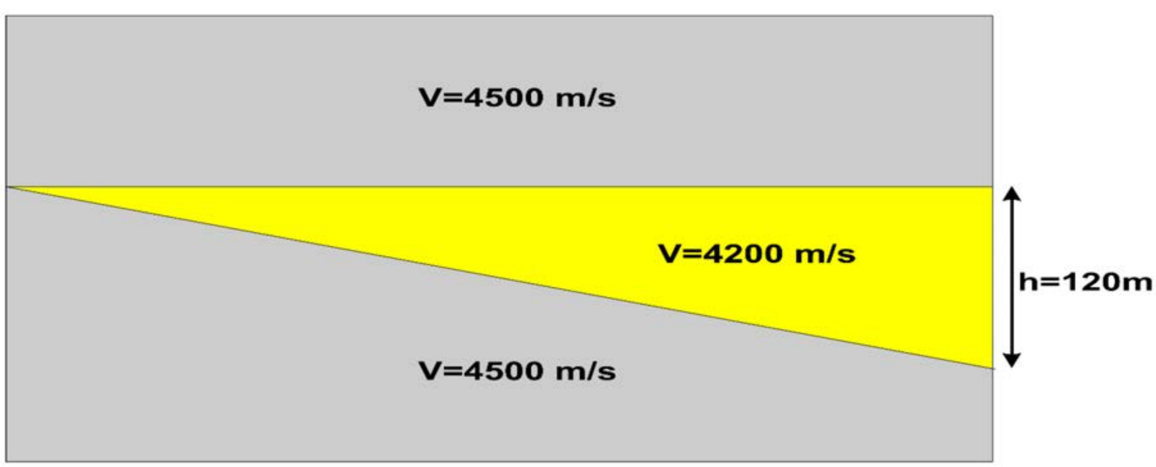

Figure 8—Clinoform velocity model

The observed amplitude maxima for the considered frequencies correspond in thickness to the signal resolution value (1/4f, with a two-way-time shown in the graphs 1 / 2f) for each of the central frequencies. When the wedge thickness is less than the resolution, the amplitude decreases as a polynomial function. These thicknesses are of interest from sandstone thickness quantitative prediction point of view based on the spectral decomposition results (Figure 9). The forecast of reservoir thicknesses exceeding the resolution in this article is not considered and can be calculated using other interpretation techniques.

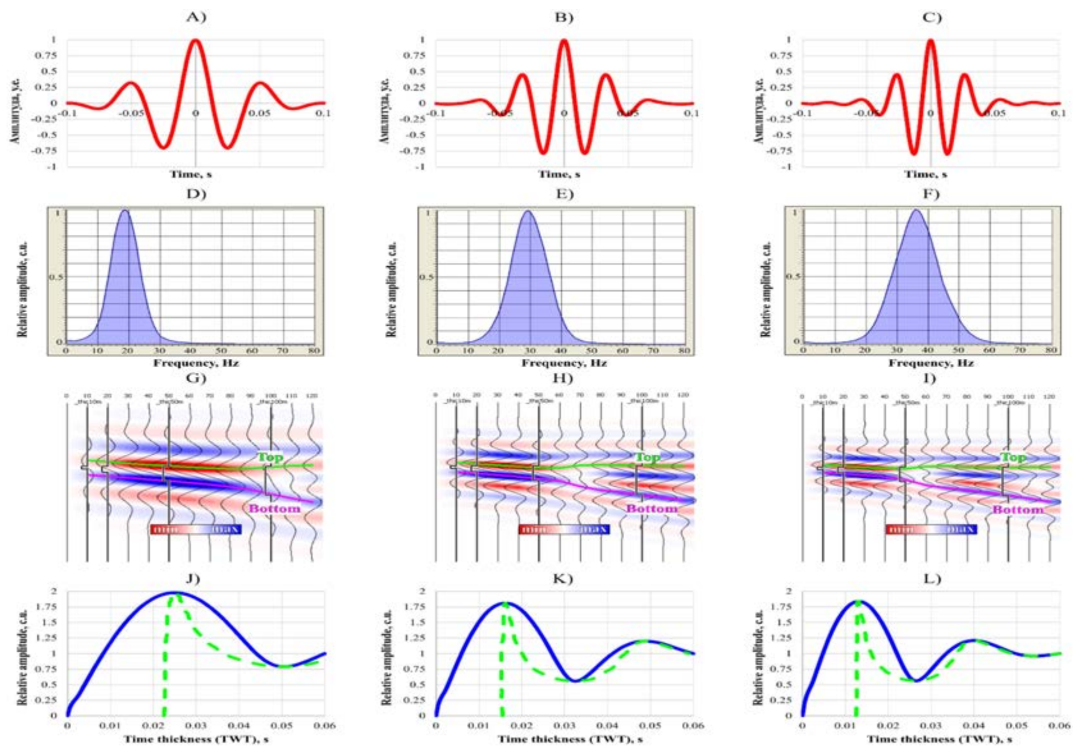

Figure 9.—The application of the extracted wavelets along the spectral composition attribute cubes with a frequency of: A) 19.4 Hz (further 19.4 Hz) B) 31 Hz (further 31 Hz) C) 41 Hz (further 41 Hz) to perform the simulation. The amplitude-frequency characteristics of the analyzed wavelets are presented: D) 19.4 Hz D) 31 Hz E) 41 Hz; synthesized wedge models using wavelets: G) 19.4 Hz H) 31 Hz I) 41 Hz; amplitude response (expressed in relative values) from the top of the synthetic wedge model obtained by convolution with signal K) 19.4 Hz L) 31 Hz M) 41 Hz

Let's describe the response curve of relative amplitudes along sandstone top using the example of a frequency of 19.4 Hz.

The resolution for this frequency (taking into account two-way time) is about 0.025 s. The maximum relative amplitude from the reservoir top is observed at this time thickness. This value corresponds to the maximum relative amplitude along top layer. It is also boundary in the further solution of the inverse problem of quantitative restoration of the wedge thickness. In order to make the transition to a numerical solution of the problem, we approximate the distribution function of the amplitudes by a second-degree polynomial by the least squares method (Figure 10).

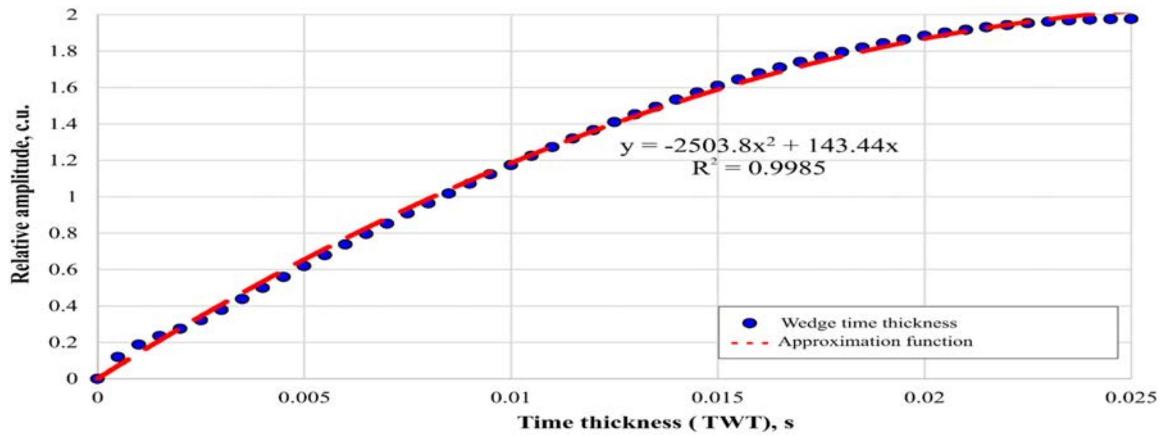

Figure 10.—Dependence of the amplitudes on the double wedge time thickness approximation and second degree polynomial by the least squares method

The resulting equation confidently describes the dependence of the relative amplitude along the wedge top on the time thickness of the wedge, expressed in two way time. The further problem is to find the inverse relationship. It is necessary to solve the resulting square equation, one of the roots of which is the value of the thickness function (TWT) by the argument of the relative amplitude along wedge top. The search for this solution is an incorrect task, since there is no uniqueness of the analytical solution, which is clearly demonstrated in Fig.6. Therefore, the value of the amplitude of 1.6 corresponds to two values of the wedge time thickness (TWT): 0.015 s and 0.035 s. However, due to the involvement of a priori information, it is possible to choose one of the two existing solutions.

In case of simulation, the thickness value is known that does not exceed the resolution of the signal. When performing the calculation using 3D seismic data, a priori thickness information is available, both from the time thickness map between the top and the bottom of the reflecting horizons (sandstone net thickness rough estimate in the view that the reservoir between the reflecting horizons is composed exclusively of sandstones) and from the well-logging interpretation data.

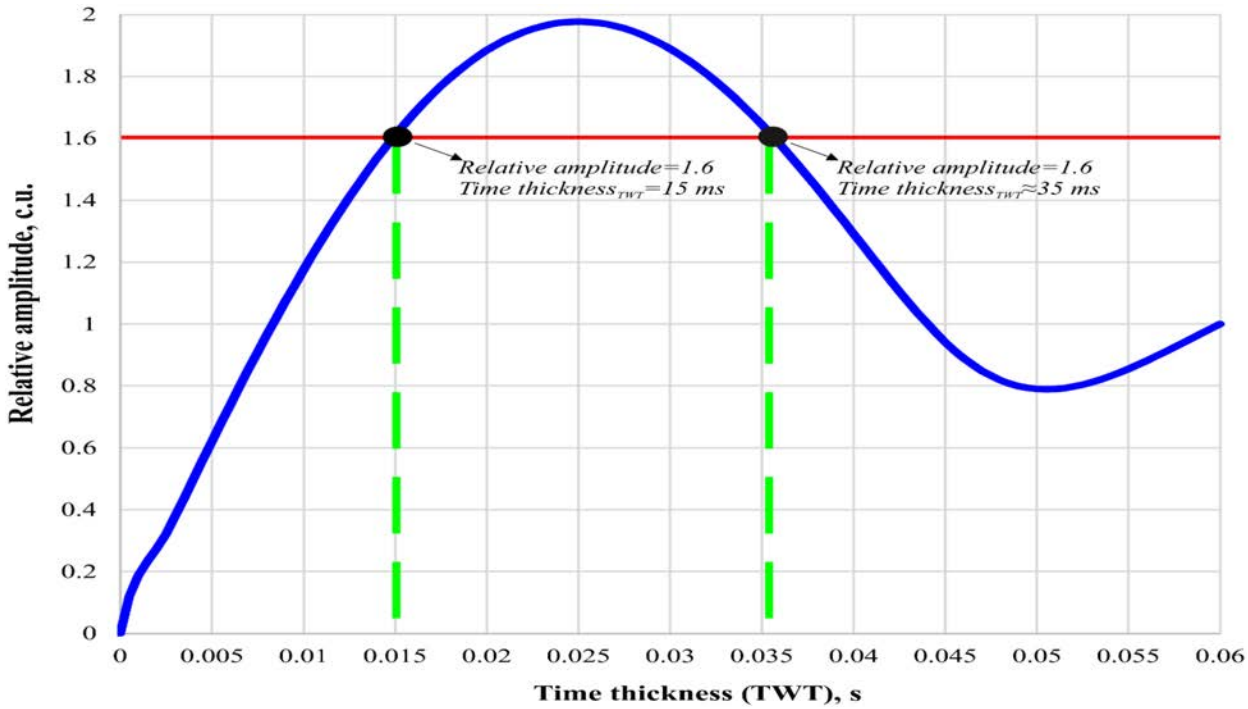

Figure 11.—Incorrect solution to the inverse problem. One time value (red line of 1.6 values) corresponds to two thickness values (green lines of 0.015 s and about 0.035 s)

We give the correct solution to this equation, satisfying the condition of the problem:

$$Time\ thickness_{TWT} = \frac{143.44 - \sqrt{(143.44)^2 - 4 * 2503.8 * Relative\ amplitude}}{2 * 2503.8}$$

The obtained dependence approximates the real thicknesses of the wedge model quite well – the maximum deviation is 1.9 MS (TWT). Using correlation of the top and bottom of the wedge model and building a time thickness map, its maximum deviation from the true value is 22.5 MS (TWT) (Figure 12).

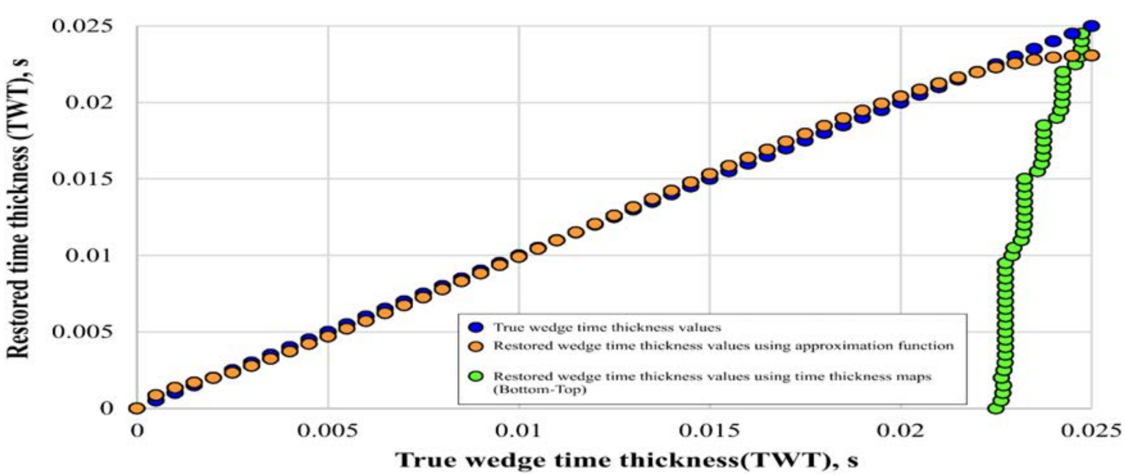

Figure 12.—Comparison of the restored time thickness values of the wedge synthetic model (taking into account double time) using the approximating solution function and using the time thickness map

Similar operations performed for models with center frequencies of 31 Hz and 41 Hz.

Based on the results of the transformations, three data arrays were obtained with information on the restored time model thicknesses (taking into account two way time). The data set of restored thicknesses must be combined into a single array. To solve this problem, it is proposed to use the existing values of amplitudes and restored values of time thickness. Let's turn to the integrated amplitude-frequency characteristic of the model in the field of considered frequency values (Figure 13).

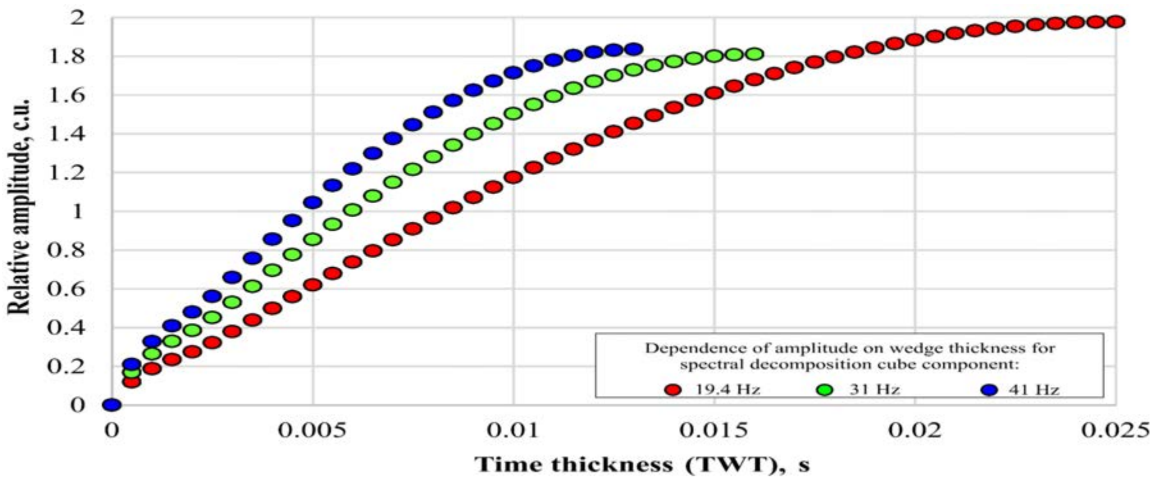

Figure 13.—The complex amplitude-frequency characteristic of the wedge synthetic model, reflecting the contribution to determining wedge thickness with individual weight coefficients

Note that each frequency component contributes to determining wedge model thickness with an individual weight coefficient. The wedge thickness value of 0.010 s (taking into account two-way time) can be calculated using all the considered frequency components. However, this thickness appears in the form of different amplitude values for each center frequency. Therefore, it is necessary to determine quantitatively how each analyzed amplitude-frequency characteristic affects the scale of the object being studied. Let h_i – be the point of the wedge model recovered thickness characterized by the amplitude response A_i for the center frequency of the synthetic model f_i. Then the wedge model net thickness can be expressed using the following law:

$$H \ni \Phi = \frac{\sum_{i=1}^{3} A_i h_i}{\sum_{i=1}^{3} A_i}$$

The calculation of the net thickness of the wedge model using the weight coefficients of amplitudes is shown in Figure 14. The maximum error in determining the thickness of the wedge model was 1.9 MS.

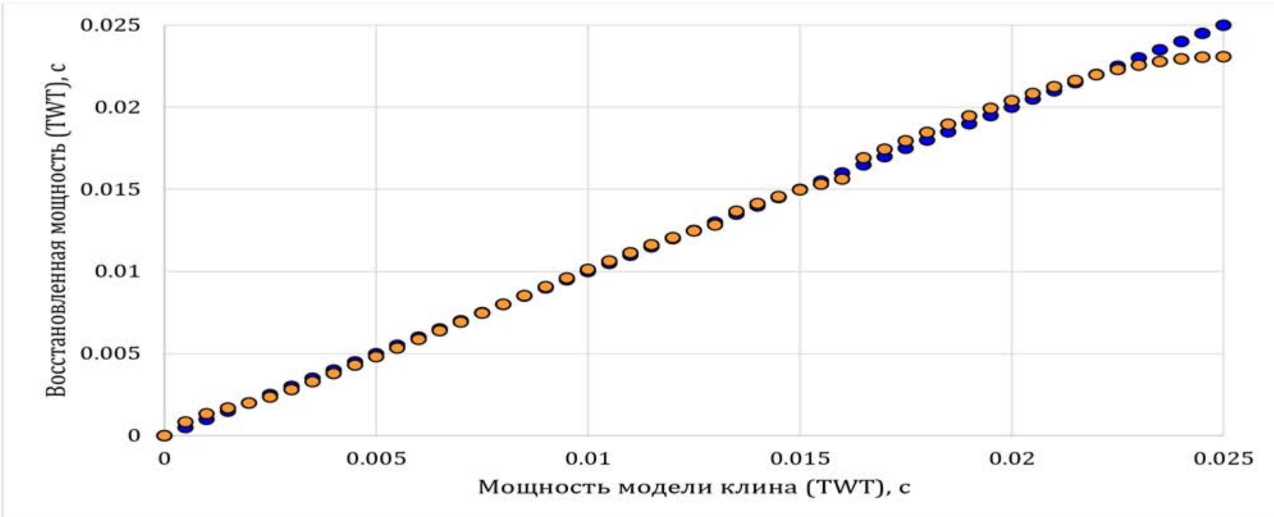

Figure 14.—Synthetic wedge model time thickness calculation using a set of frequency components arrays

The possibility of performing a quantitative prediction based on the results of spectral decomposition is clearly demonstrated on model materials. What is the applicability of this method for field materials of mogt-3D seismic survey? Let's consider this question on the example of the designated object of research- the Achimov clinoform complex submarine fan.

Case study

The described methodic was tested on an Achimov clinoform deposits of a field X. According to an oil and gas geological zoning this field is located in a Pur-Tazov oil\gas-bearing area in West-Siberian oil and gas province. The 3D seismic survey of 520 km^2 was performed at a field site; within the area there are 7 wells penetrating the Achimov clinoform complex.

Achimov formation (early Neocomian) has been the subject of study for many oil and gas and service companies for many decades. These deposits have very complex geological structure along with layer thickness and grain size heterogeneity. Achimov formation genesis and details of geological structure are still a subject of discussions (Butakov M.V., 2018).

Perspective objects are presented with sand bodies and have similar genetic and lithological-petrophysical features. An object interpreted as a submarine clastic fan is distinguished in the area of the field X in one of the Achimov complex layers as a result of an integrated analysis of the geological and geophysical data.

Wavefield analysis shows an anomaly with high amplitude and lower frequency. The calculated maps of the attributes "amplitude envelope" and "instantaneous frequency" allow us to confidently outline the submarine clastic fan (Figure 15 - Figure 16).

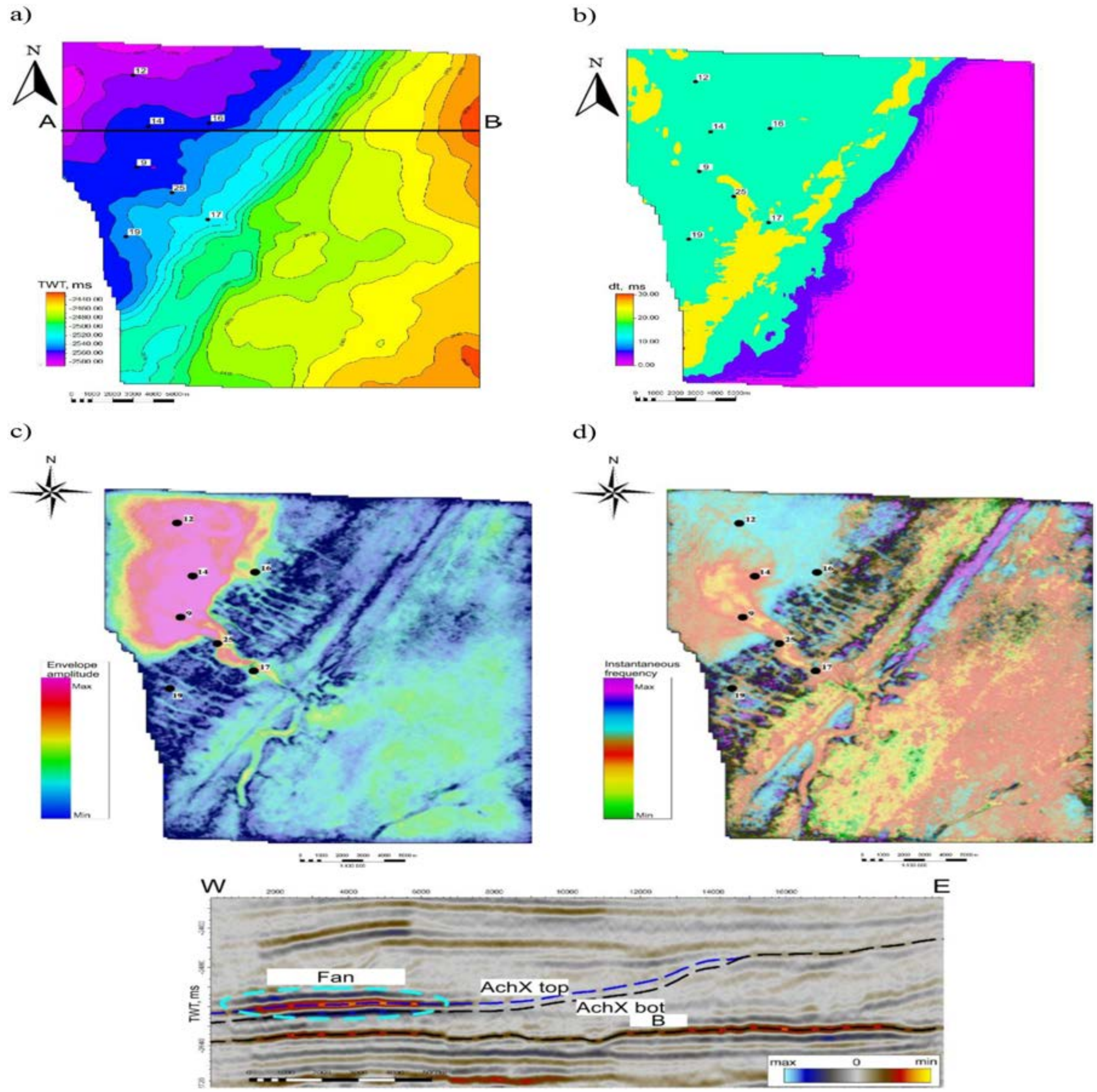

Figure 15.—Time map (a), Time thickness map (b), envelope amplitude (c), instantaneous frequency (d) of AchX layer, time section in the interval of achimov formation.

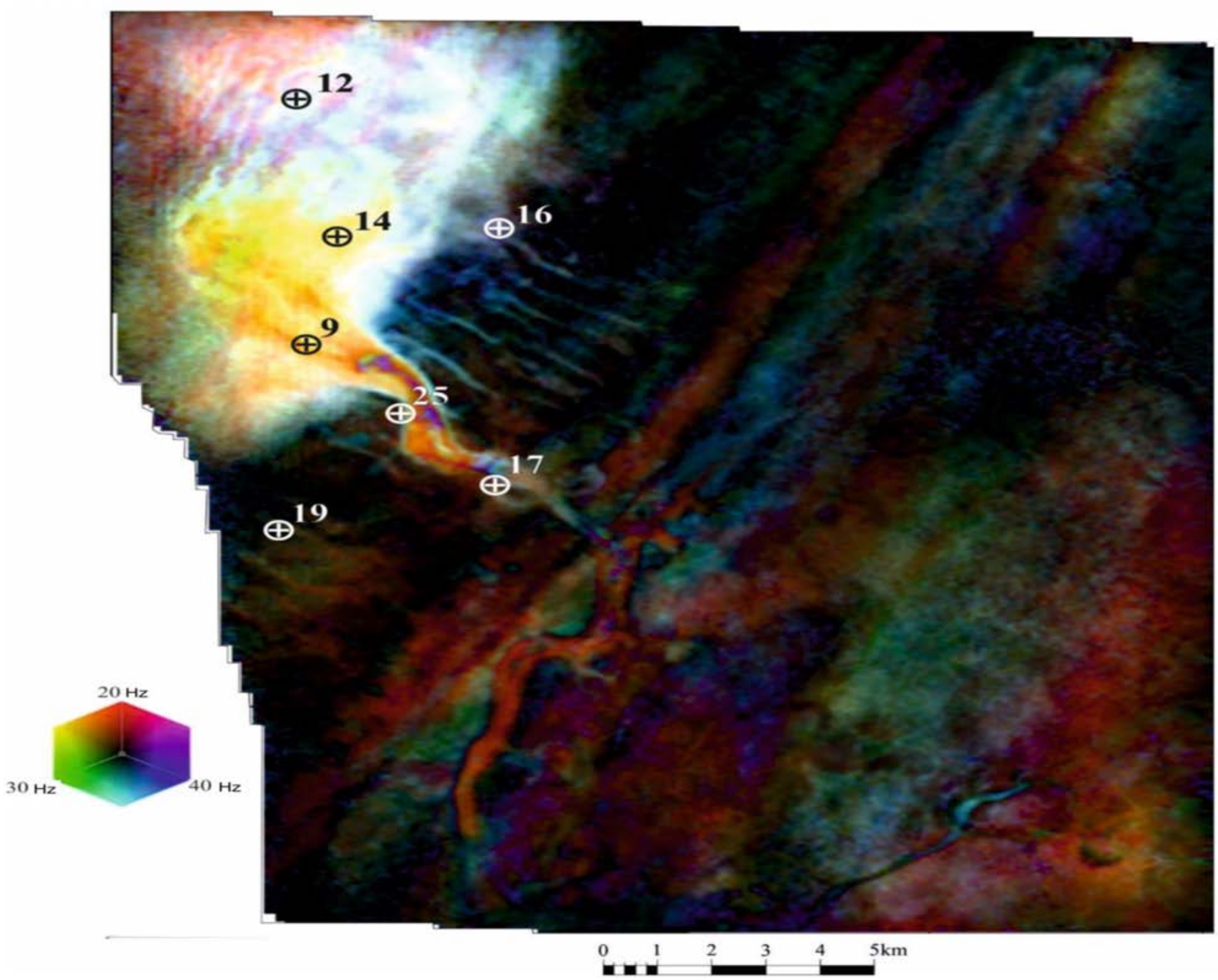

Figure 16—AchX spectral decomposition attribute map

4 out of 7 wells that penetrate this object confirmed presence of sandstone and hydrocarbon saturation. According to the core description the reservoir consists of gray fine-grained sandstone, less often coarse-grained and siltstone. According to well log data interpretation results sandstone reservoir thickness varies from 6.7 to 28.1 meters. Based on the average sandstone velocity calculated from the acoustic logging the time thickness of the sand deposits was estimated (Table 1).

Table 1—Initial data

Well	Sandstone thickness (m)	TWT thickness (s)
12 (1)	28.1	0.0134
16 (2)	6.7	0.0032
14 (3)	21.1	0.0100
9 (4)	24.5	0.0117
19	0	0
25	0	0
17	0	0

In addition, in this area there are 3 wells which didn't penetrate the sandstone reservoir, these wells can be used as a verification of the presented methodology result.

Spectral decomposition qualitative interpretation results

Lower cretaceous (neocomian) deposits of West Siberian basin consists of a widely known clinoform complex presented by lateral accretion deposits. Clinoform structure of a neocomian deposits is very well captured by seismic sections.

Clinoform package is usually broke down to three parts: topset (undeform), foreset (clinoform) and bottomset (fondoform). Foreset part, which corresponds to a slope deposits consists mainly of clay-rich rocks. Topset and foreset parts consist of interbedded sand and clay layers. Bottomset sand deposits are known as Achimov formation. It has assumed that Achimov formation is formed during clastic influx increase when a significant part of sand material bypasses slope area and being transported to deep-water area by turbidity currents (Bazel A.L., 2010).

In the field X site topset deposits are shallow marine and foreset and bottomset are estimated of approximate 300-350 m of paleodepth.

Integrated seismic attribute analysis and spectral decomposition was performed to locate paleo-channels, which can potentially be oil/gas traps.

Maximum thickness of clinoform bodies corresponds to a foreset (clinoform) part and reaches approximate 56 m. In a bottomset part thickness gradually decreases.

With that said, we can conclude that Achimov sand deposits were formed during an active alongshore sediment transport with a single clastic influx source from a river delta. This is a traditional genetic model for Achimov formation (Nezhdanov A.A., 2000). The most perspective zones are local depocenters (local thickness maximums) of Achimov sandstones which have better reservoir characteristics (Figure 17).

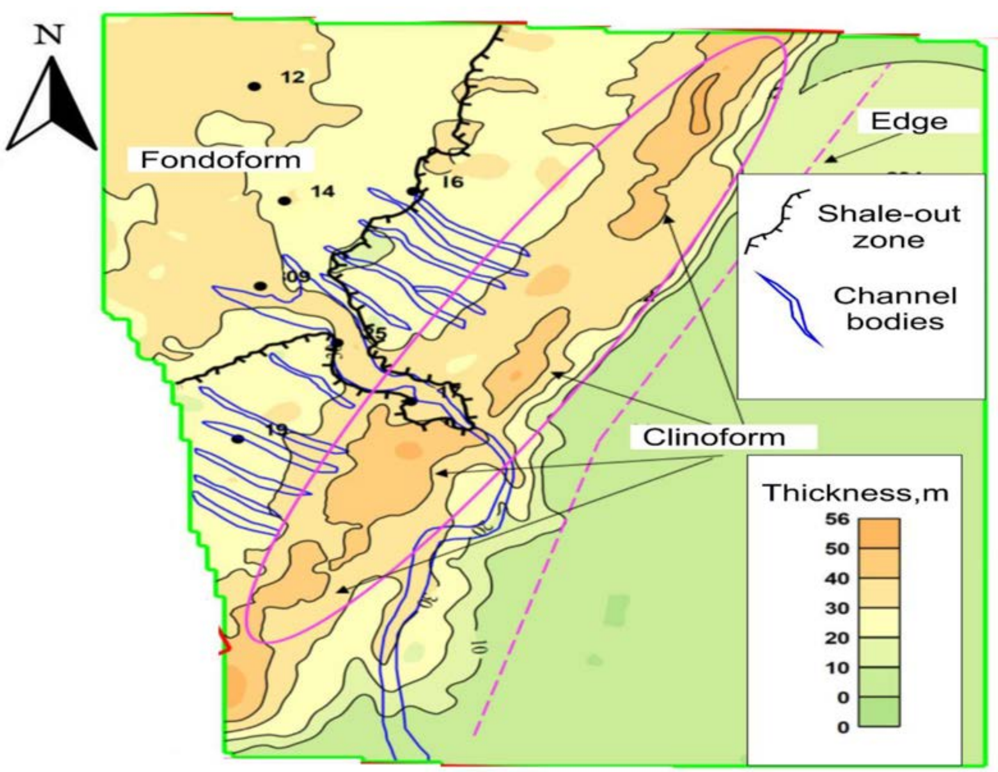

Figure 17.—AchX total thickness map

Ideal sedimentary trend method was used to improve understanding of Achimov deposits structure and localize sand bodies (Nezhdanov A.A., 2017).

Ideal sedimentary trend method involves analysis of thickness deviation from ideal clinoform thickness calculated assuming the same sedimentation conditions along the coastline. The same sedimentary conditions include equal sedimentary influx rate, equal slope characteristics and equal subsidence rate. Zones with thickness being less than ideal trend are interpreted as sediment starvation zones. Zones with thickness being greater than ideal trend are interpreted as local depocenters with increased sand thickness (Nezhdanov A.A., 2017).

Ideal sediment trend is mapped based on a set of thickness isolines built from an ideal shoreline, which was copied along the main transport direction with thickness values assigned from smoothed thickness map.

Thickness deviation from an ideal trend for AchX formation is shown on a Figure 18.

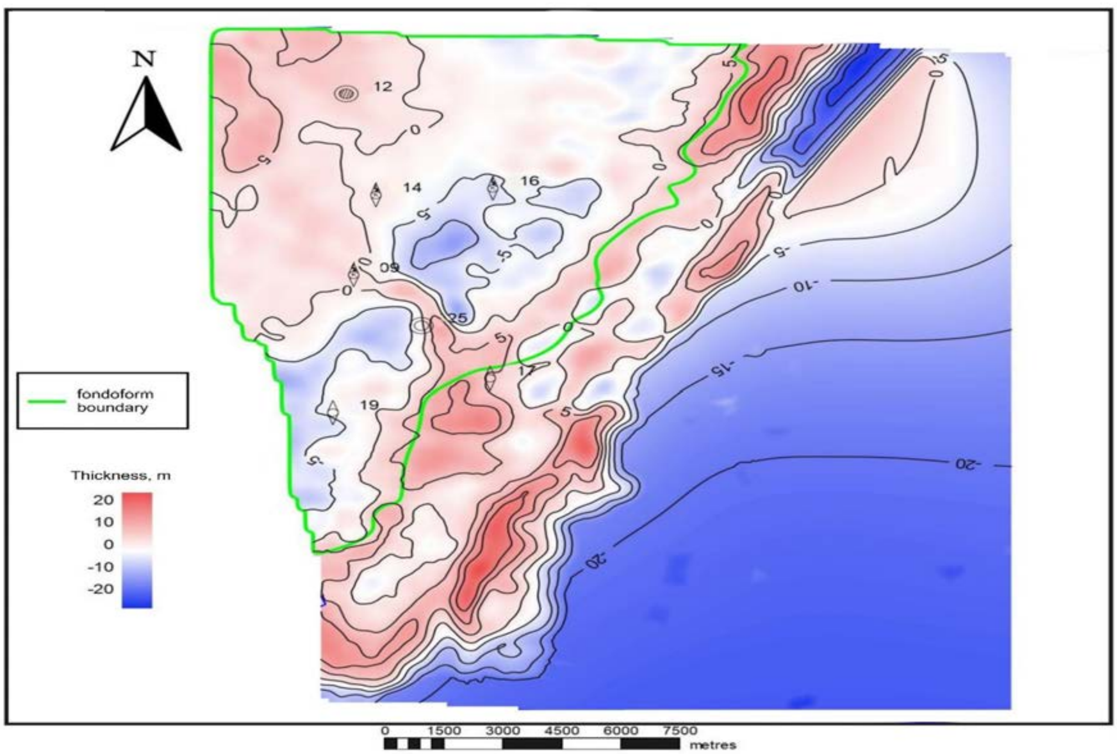

Figure 18.—AchX difference map between total thickness and ideal trend

Three main zones with increased thickness are determined in AchX formation. Two of them are located in southwest and northeast parts spreading out from southwest to northeast part of the area and were formed in continental river condition along the shoreline. The third depocenter is located in in northwest part of the area the bottomset zone and is formed due to deepwater fan deposition. Between these depocenters an area of decreased thickness is determined, which corresponds to a slope bypass zone.

To summarize the described submarine fan has the following features: shelf zone, slope zone, deepwater zone, submarine channel and submarine fan. Sand bodies were formed during regression periods when the shelf was drained, and mass transfer processes (landslides, mud flows, and turbidite flows) took place on the slope. Channels supplying clastic sediments transport to the deepwater area are well established in the wavefield. In the transgression periods sedimentary influx is mainly presented by clays which lead to a Achimov sand bodies being separated by clay layers (Figure 19).

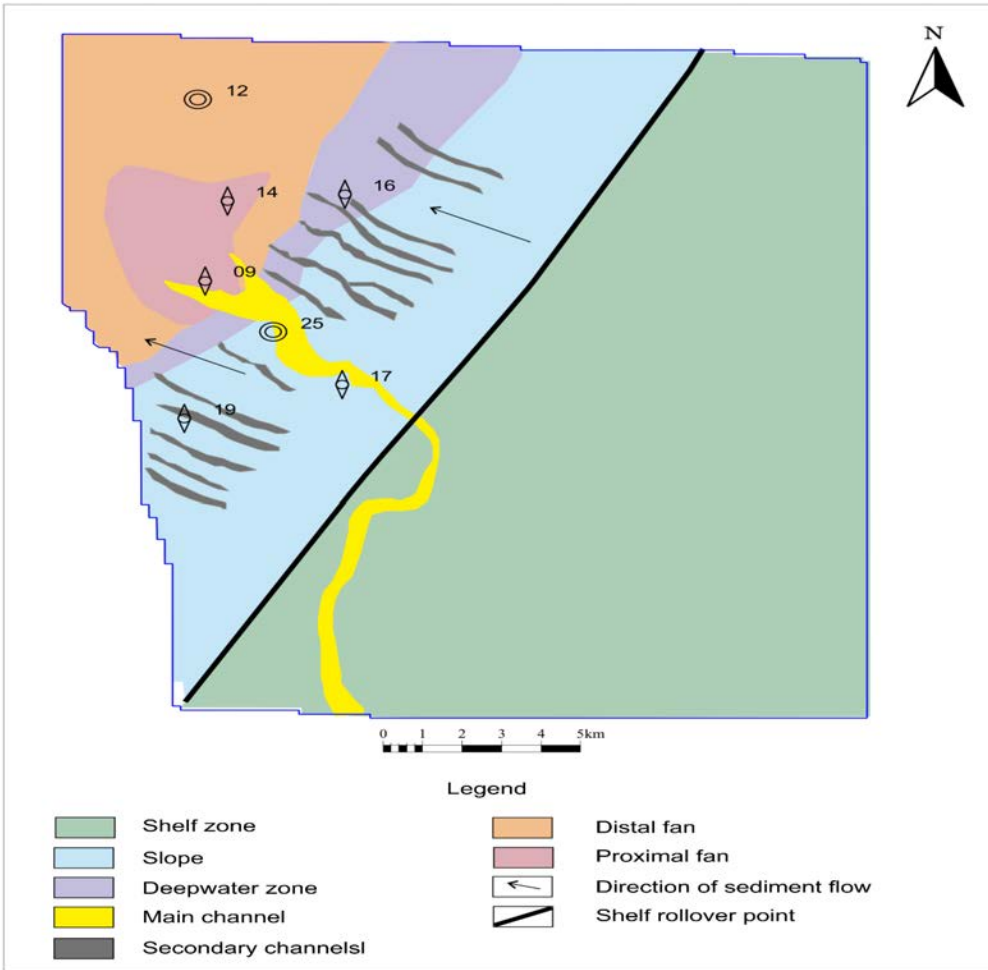

Figure 19.—AchX layer facial scheme

The calculation methodology

The method of predicting quantitative characteristics of the geological structure of the section based on the results of spectral decomposition, which was considered on synthetic data, was intended for contrasting objects in the field of acoustic impedance. The studied sand body, interpreted as an underwater cone of the Achimov clinoform complex, satisfies this condition. Nevertheless, it is necessary to determine as assumptions some differences between the object of research and theoretical representations. The construction of the previously presented wedge seismic model based on the uniformity of the lithological composition and physical properties of the reservoir rocks and wedge rocks. Interpretation of the reflecting horizons of the top and bottom of the studied formation also involves tracing top and bottom of sand deposits. However, the reservoirs of the Achimov formation represented by an interlayer of sand-clay interlayers, which means that the lithological composition and physical properties of the wedge model are heterogeneous in approximation to field materials.

It is also necessary to take into account that the study should be performed on a seismic scale that does not exceed the maximum value of the resolution. In this case, consideration medium is microscopically inhomogeneous, but macroscopically homogeneous with effective properties. Therefore, the task of quantitative prediction of spectral decomposition results is to search the net thicknesses of sand bodies in the Achimov clinoform complex.

19,4 Hz. According to the simulation information, for a frequency of 19.4 Hz value of the resolution limit (taking into account two-way time) it is about 0.025 s. By comparing this value with a priori well-logging data (Table 1), it is possible to assume that thickness of the interpreted underwater fan in interwell space will most likely not exceed the value of the threshold of the resolution of this signal. Consequently, with the existing thickness values for the central frequency of the signal of 19.4 Hz, the amplitudes will not reach the maximum of constructive interference both the synthetic wedge model and the spectral decomposition attribute map.

Working directly with the spectral decomposition attribute map provides a preliminary statistical analysis of amplitude values using the robust method. Ability to detect "outliers" values that stand out from the general sample and affect subsequent operations with amplitudes is advantage of this procedure. After calculations, the analysis removes values that exceed the values of the "external borders" of the amplitude data array. In addition, positive values of amplitudes assumed to be zero if they do not meet the conditions of the applied method. As a result, spectral decomposition attribute map prepared for further calculations.

However, it is not possible to recalculate the amplitude map for the central frequency of 19.4 Hz (Figure 20) along the studied top AchX layer using the obtained solution function in the modeling chapter due to the discrepancy between the amplitude levels of synthetic and field seismic data. In this case, we propose to reduce the amplitude map with a central frequency of 19.4 Hz to the level of relative amplitudes of the synthesized model. Standard normalization using the maximum and minimum amplitude values is not possible due to the lack of information about the maximum amplitude value of spectral decomposition attribute map. Therefore, it is proposed to estimate the values of the amplitude map in the area where wells intersect underwater fan (Table 2). In addition, based on a priori information from model data, there is an additional possibility to add a point with an amplitude value of 0 to the cross correlation relationship, which corresponds to the absence of sandstone's net thickness.

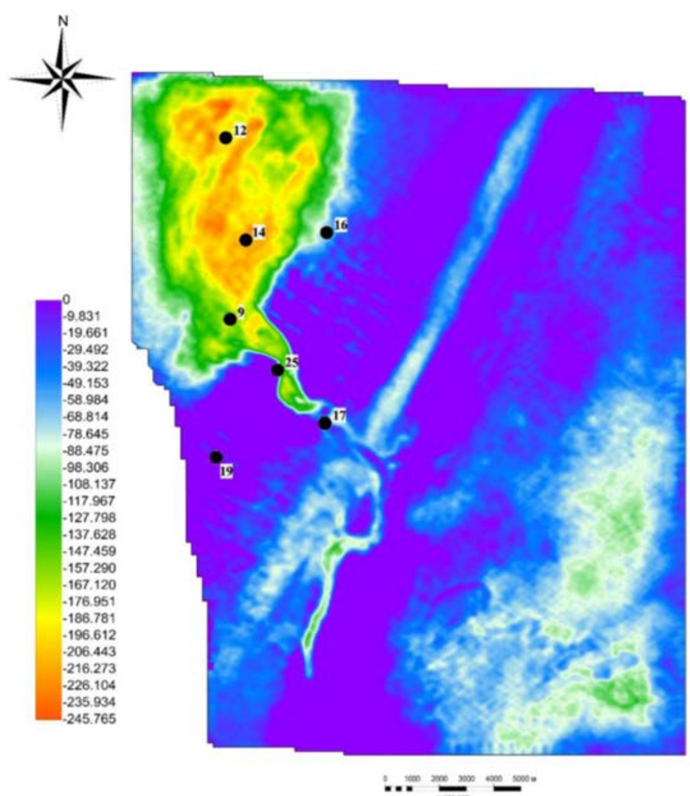

Figure 20.—Amplitude map (from 19,4 Hz cube) along AchX top horizon

Table 2—Model and real amplitudes comparison

Well	Amplitude along AchX layer, c.u.	Net thickness, m (well data)	Time thickness (taking into accout TWT) at Vp=4200m/s, s	Wedge model relative amplitudes, c.u.
12	191.712	28.1	0.0134	1.5029
16	73.3	6.7	0.0032	0.4557
14	215.3	21.1	0.0100	1.2288
9	157.8	24.5	0.0117	1.3703
Priori information	0	0	0.0000	0.0000

Let's move on to finding the normalization coefficient. To do this, it is necessary to evaluate the dependece graph of relative model amplitudes along the wedge top and spectral decomposition amplitude map along the AchX top layer (Figure 21). As it was emphasized earlier, for model and field data, the distribution of amplitudes for their corresponding thicknesses, which do not exceed a quarter of the signal period, is described in an idealized representation by a polynomial of the second degree. Therefore, there is a linear dependence between the two data sets, which is the normalization coefficient for the spectral decomposition attribute map (Figure 22). Reducing the amplitude values to a single range allows further calculation of the sandstone's time thickness using the previously obtained dependence based on the results of modeling (Figure 23).

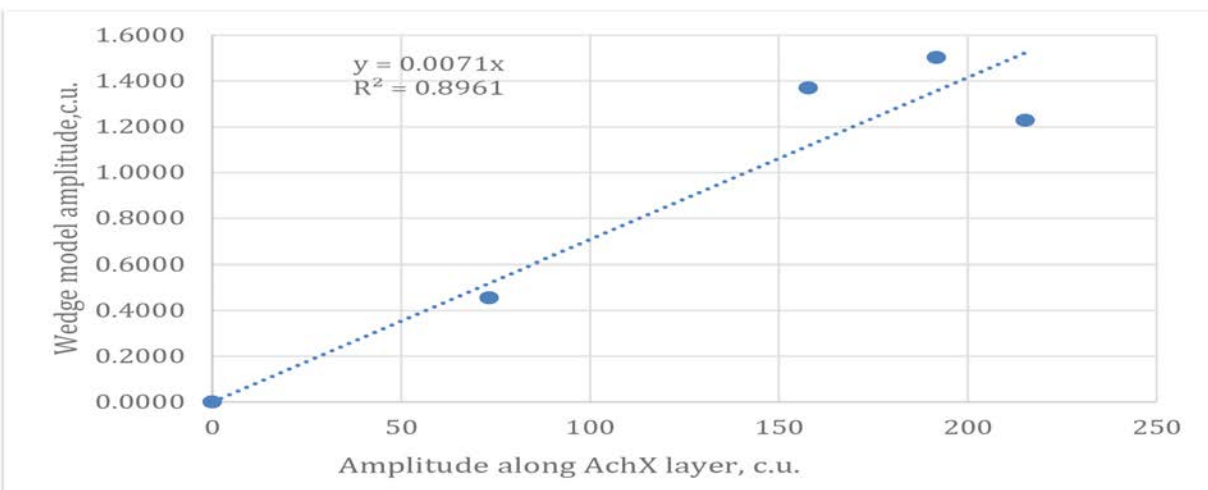

Figure 21.—Crossplot amplitude model values versus amplitude along AchX top layer

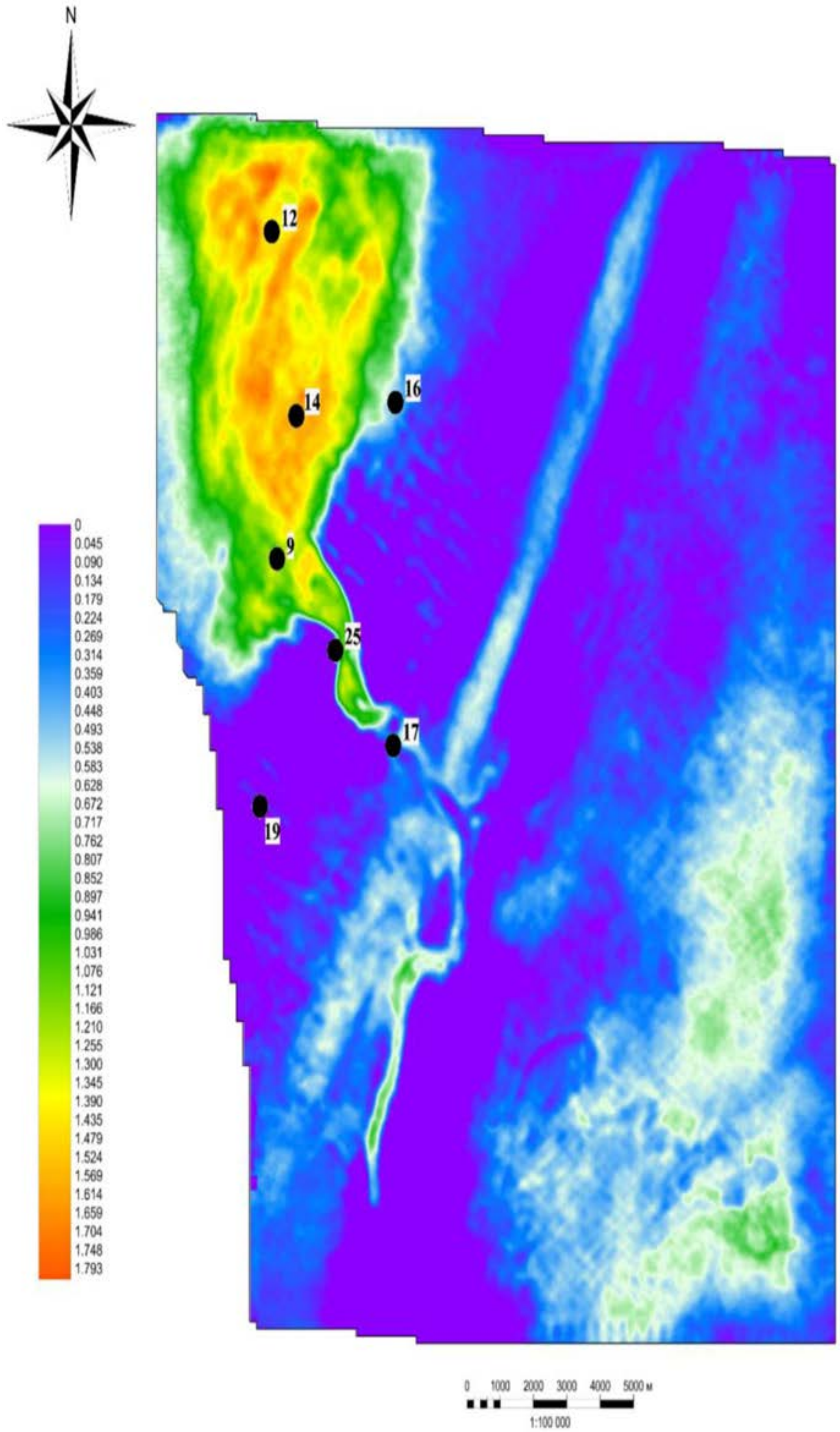

Figure 22.—Normalized amplitude map along AchX top layer

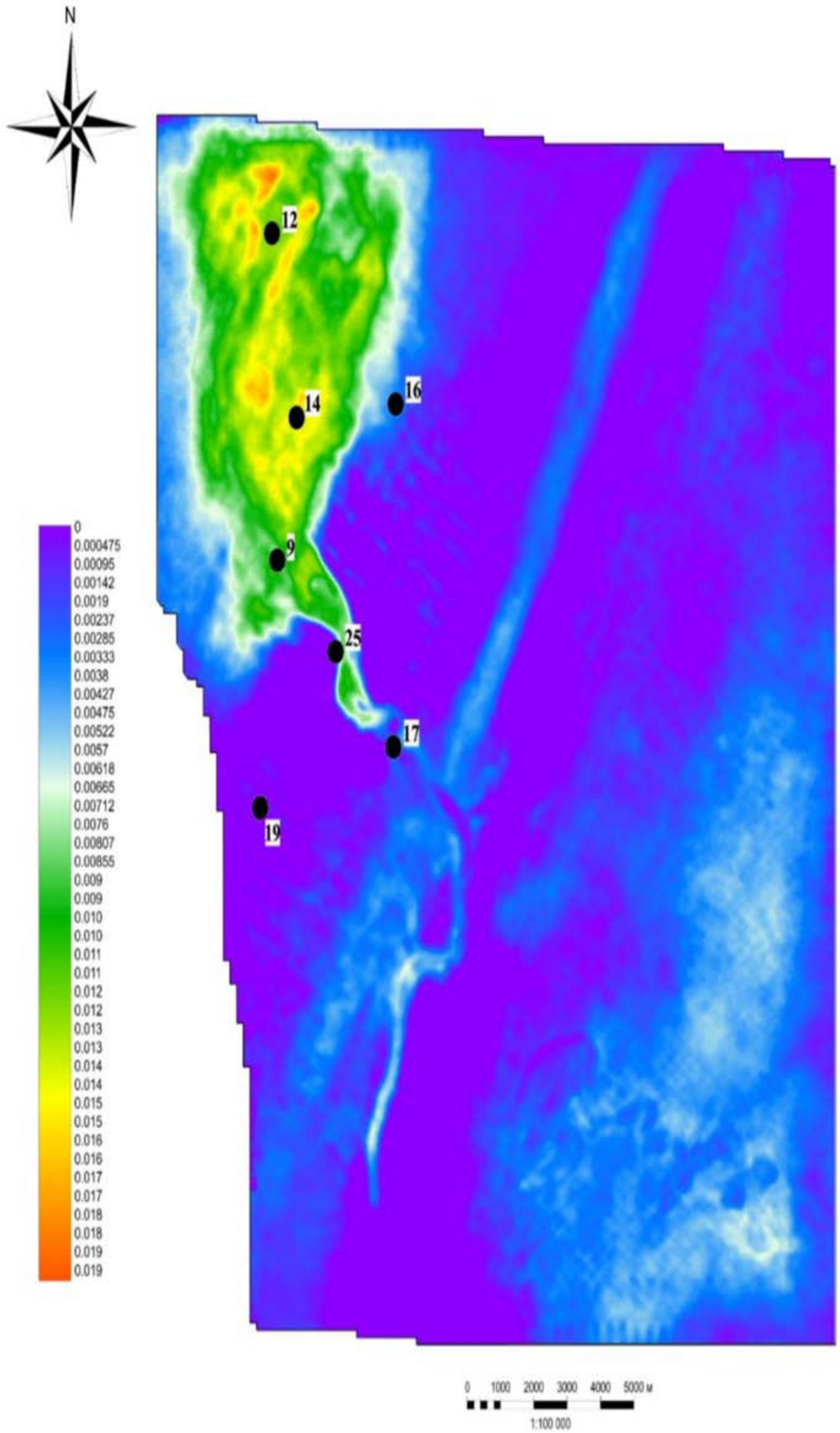

Figure 23.—Time thickness map (TWT) of AchX sand deposits for 19,4 Hz frequency

A comparison of results obtained from the restored time thickness map (taking into account two-way time) for the central frequency of 19.4 Hz and the well data presented in Table 3.

Table 3—Quality Control

Well	Time thickness (at velocity 4200м/с) (TWT), с	Restored time thicknesses (TWT), s	Net thickness, m (well data)
12	0.0134	0.012	28.1
16	0.0032	0.004	6.7
14	0.0100	0.014	21.1
9	0.0117	0,009	24.5
17	0	0.001	0
25	0	0.001	0
19	0	0	0

The maximum deviation time thickness from the well data is 2 ms.

The results analysis of spectral components maps does not stop here. It is necessary to carry out a similar sequence of actions to identify and quantify small thickness objects, when considering spectral decomposition attribute maps with a central frequency of 31 Hz and 41 Hz.

However, the main difference is the use of restored time thickness map obtained at the previous research stage when performing operations with maps. For example, if the values of the restored time thickness in interwell space are equal or greater than ¼ of the signal period, it is possible to perform an analysis of the spectral decomposition attribute map with the central frequency of the component up to the boundary value of its resolution. In addition, it is assumed that the maximum amplitude value on the spectral component attribute map is reached, for the value of the restored thickness corresponding to ¼ of the signal period. Therefore, normalization of this map can be performed using two values:

1. The amplitude response with a zero value in the absence of net sandstone thicknesses;
2. It is possible to compare the maximum amplitudes for model and real data with an net sandstone thickness of ¼ wave period, by eliminating the region of uncertainty in solving the inverse problems.

As a result, at the end of the spectral decomposition attribute maps analysis, three data sets of restored time thickness values were obtained (taking into account two way time), which should be combined into a single array (Figure 24). To do this, we suggest using the methodology discussed in the modeling chapter on the example of synthetic data.

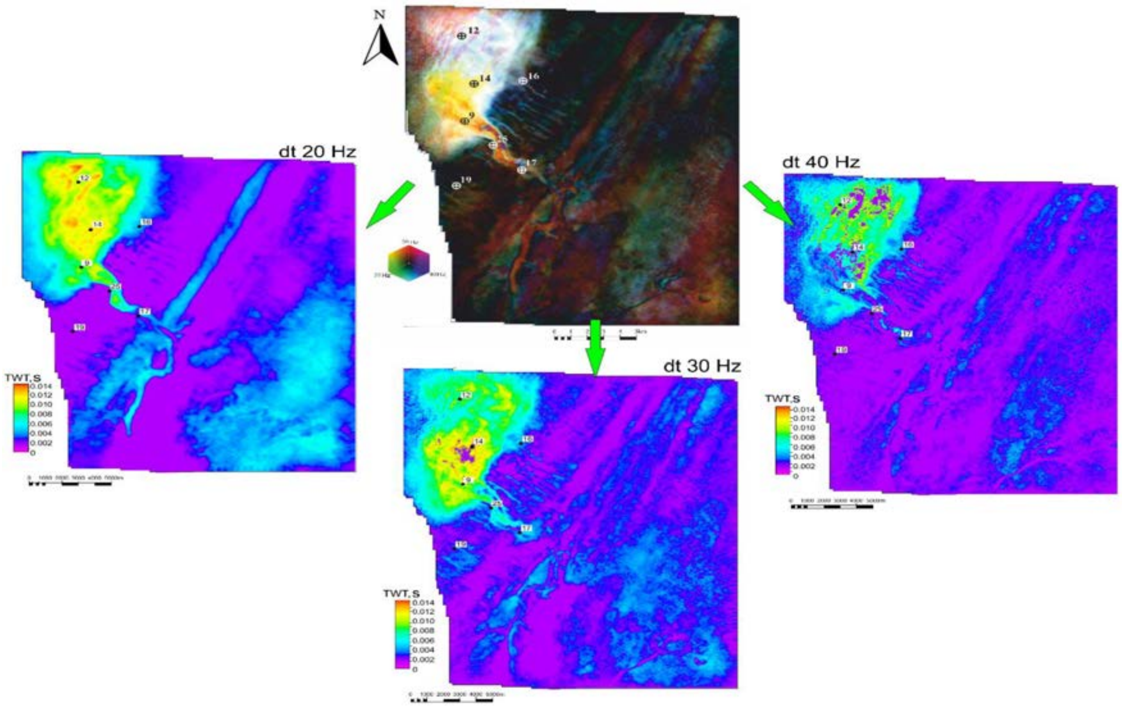

Figure 24.—Predicted thickness maps of sand deposits at different frequencies

Results

Predicted time thickness map of the AchX sandstones of Achimov formation is the result of this research (Figure 25). The resulting map reflects all main geological features in the range of formation. The alluvial fan with the inlet of AchX reservoir and smaller erosional incisions are clearly distinguished by increased values of interval times.

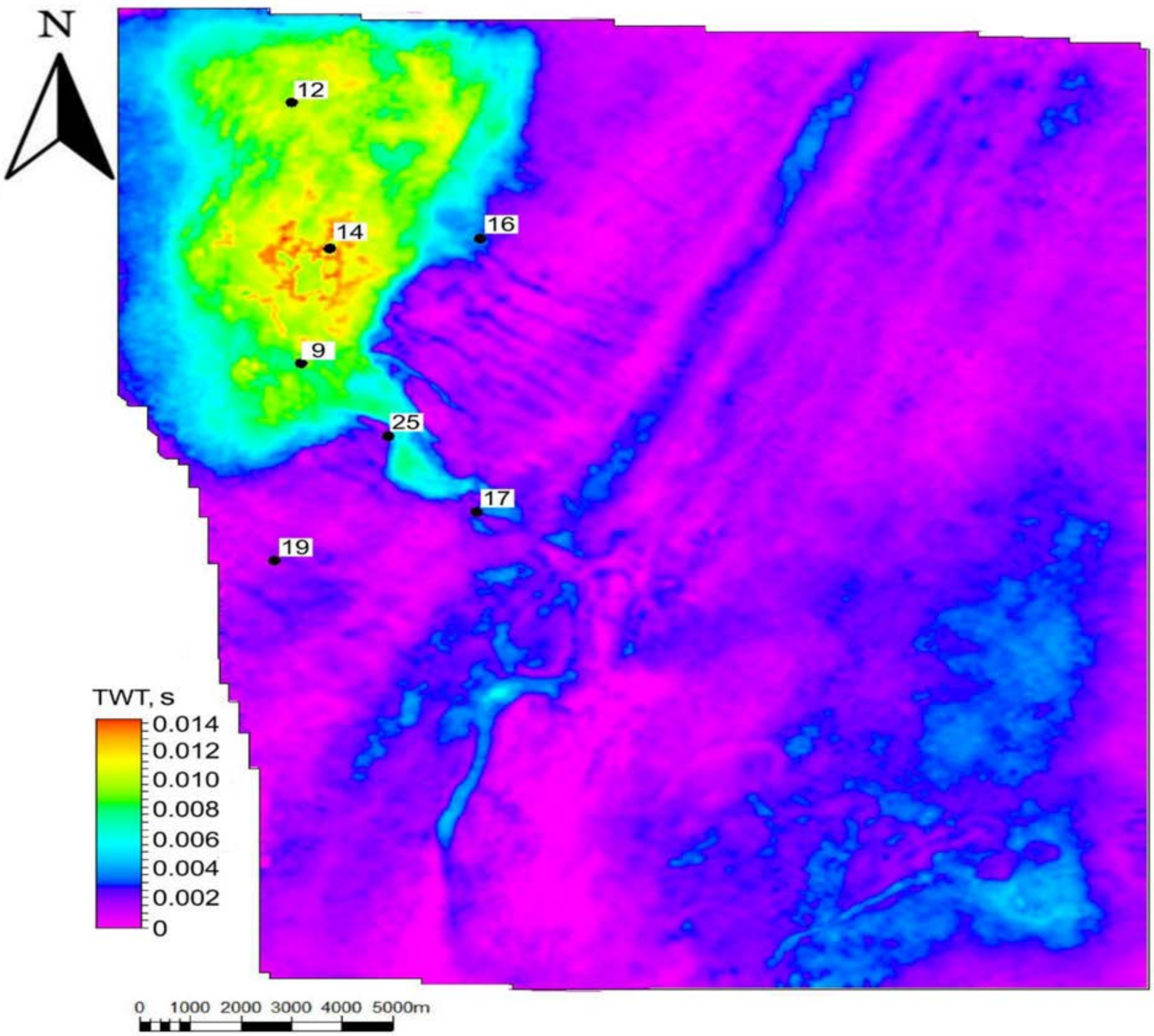

Figure 25.—AchX sandstone time thickness map by the spectral decomposition results

The entire set of available velocities was analyzed to transform time thicknesses to the depth: interval velocity cube as a result of depth migration, AchX interval velocity map by well-logging data, pre-stack inversion results (the ratio of Zp to the density cube). Each set of velocities used to obtain net thicknesses and analyzed for comparison with results of drilling. Conversions from time thicknesses to net thicknesses by seismic inversion are characterized by the smallest errors (Figure 26). Transformation results based on the values of interval velocity map from well-logging data are also close to seismic inversion results. That is explained by close nature of their obtaining. Deviations of predicted net thickness map using the interval velocity cube from depth migration may be explained by insufficient dissection of the resulting cube, which is the expected result.

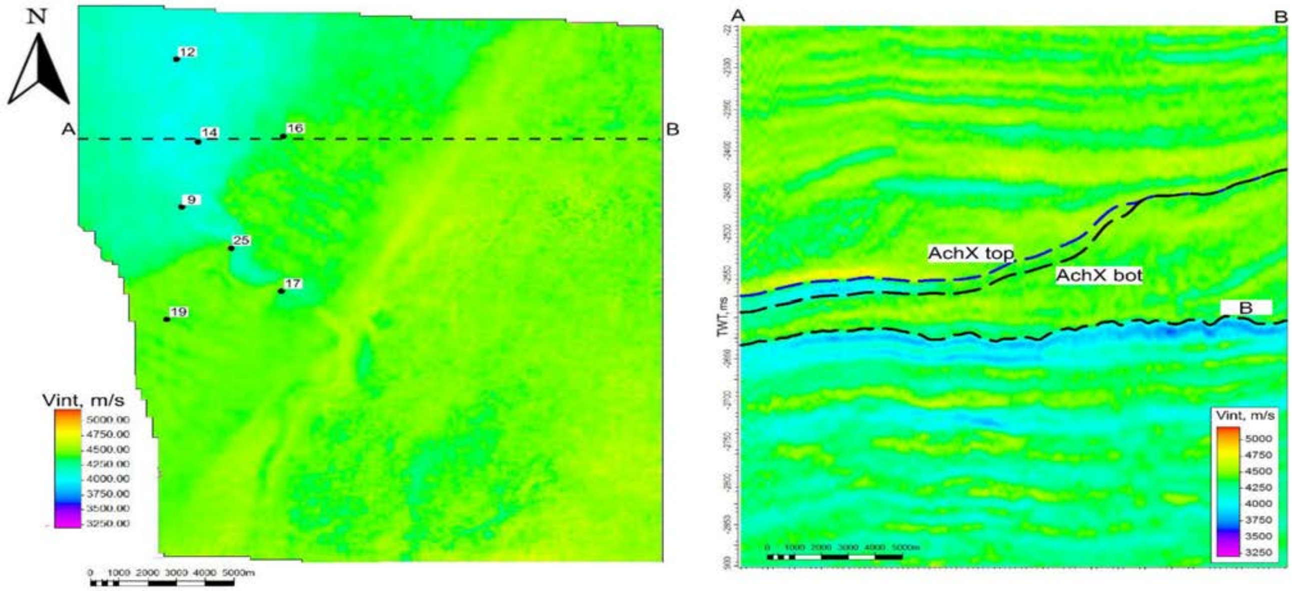

Figure 26.—Mean interval velocity map of AchX (left) and interval velocity cube time section in the Achimov formation interval (right) according to seismic inversion results

Figure 27 shows results of converting time thickness map of AchX formation sandstones into net thickness map using interval velocity cube based on seismic inversion results. Standart deviation calculation of the predicted sandstone thickness from well information, which was 4.72 m (Table 4), was a quality quantitative assessment. Comparison of predicted net thickness map of AchX sandstones, according to the spectral decomposition presented in this research to seismic inversion results, which are one of the main quantitative prediction methods, was an additional quality assessment (Figure 28). On the work area, a reliable dependence of sand deposits thickness of the studied formation on the average acoustic impedance values was obtained (Figure 29), which allowed us to obtain a net thickness map from acoustic impedance cube. Sandstone thickness maps according to the results of spectral decomposition and acoustic inversion are comparable. However, error quantitative estimation of two independent methods, based on standart deviation calculation, showed the advantages of predicting spectral decompsition results comparison with standard method of seismic (Table 4).

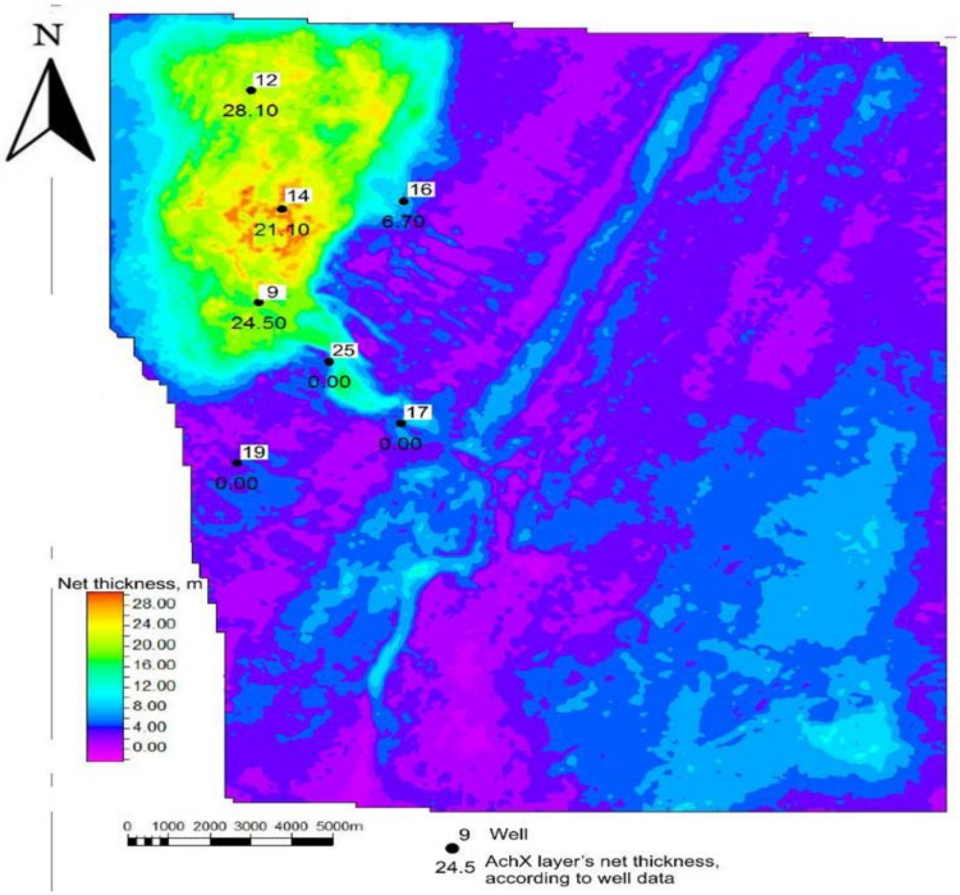

Figure 27.—AchX net thickness map predicted by the spectral decomposition results

Table 4—AchX predicted net thickness comparison between seismic inversion and spectral decomposition results

№ well.	Net thickness, m (well data)	Acoustic inversion		Spectral decomposition	
		Net thickness, m	Difference with well data, m	Net thickness, m	Difference with well data, m
9	24.5	24.47	0.03	19.85	4.65
12	28.1	20.92	7.18	21.33	6.77
14	21.1	24.07	-2.97	21.93	-0.83
16	6.7	4.76	1.94	7.78	-1.08
17	0	5.57	-5.57	4.64	-4.64
19	0	-5.06	5.06	2.75	-2.75
25	0	5.67	-5.67	6.14	-6.14
Standart deviation, m			5.05		4.72

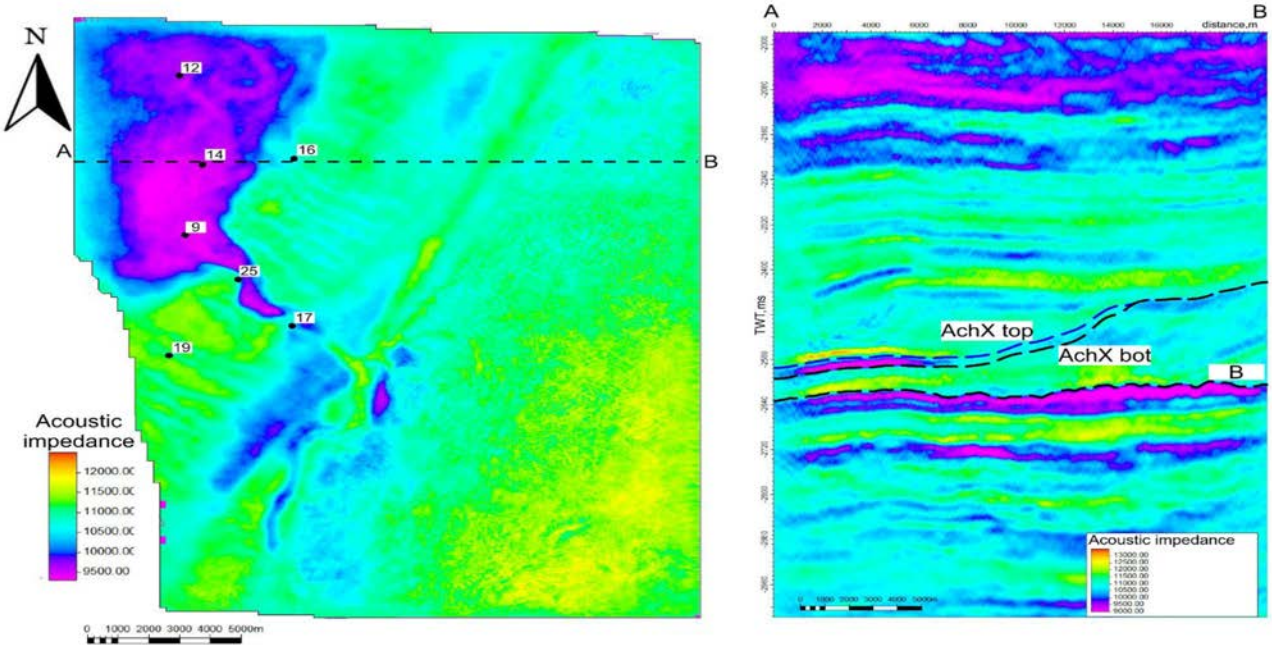

Figure 28—Mean acoustic impdenace map of AchX (left) and acoustic time section of impedance cube in the Achimov formation interval (right)

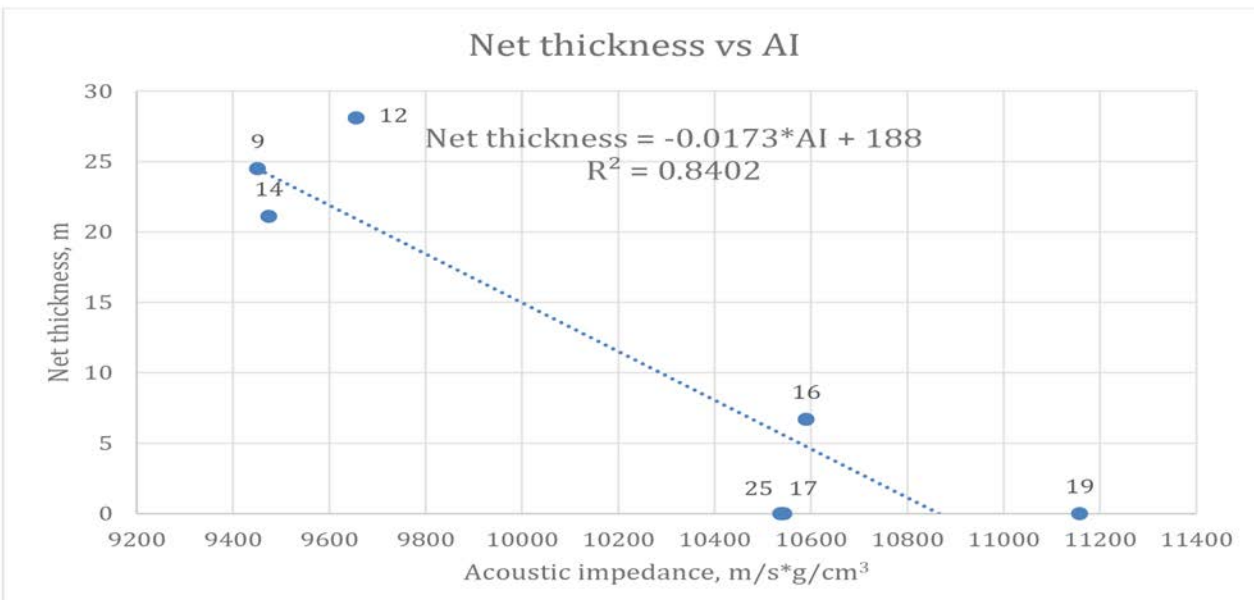

Figure 29—Crossplot net thickness versus P-impedance of AchX layer

Conclusions

Methodology is proposed for using the spectral decomposition results to predict the sandstone thickness, based on research results carried out on the example one of Achimov formation layers. The proposed technique can be used both in conjunction with traditional methods of quantitative dynamic interpretation, and separately from them. For example, when seismic inversion results cannot be directly used for quantitative prediction.

The main advantages of the proposed methodology include the possibility of obtaining maps of the predicted sandstone time thickness for objects not penetrated by wells, despite the difficulties in normalizing amplitudes that arise in this situation. In addition, there are prerequisites for successful testing of the presented approach on little studied and probably not studied by drilling areas using a complex of certain interpretative techniques.

It should also be noted that one of the advantages of the methodology considered is the minimum amount of input data, which essentially allows you to get a result that is almost independent of the quality and quantity of the source information. An exception in this case can only be the quality of seismic materials and correlations of reflecting horizons. Thus, the result obtained has grounds to be considered in the process of dynamic interpretation of seismic data as an additional source of information about the reservoir properties.

In the considered example, prediction results of AchX layer net thickness according to spectral decomposition turned out to be more accurate than the prediction made using seismic inversion. That fact, transfers spectral decomposition method from the category of qualitative attribute analysis to a full-fledged method for quantitative prediction of reservoir properties.

Acknowledgments

The authors of the article are grateful for the consultation, provision of materials, as well as technical and professional support in the process of writing the work:

- GeoGrid Geological Data Research Center LLC (Moscow) represented by the Chief Executive Officer Ph.D. Bolotov S.N. and Chief Operations Officer Miletskaya G.V.
- Gazpromviet LLC (Moscow) represented by General Director Krasnikov I.Y and Chief Geologist – Deputy General Director Denisov Y.I.

References

1. Beisel A. L. The tectono-sedimentary complex is the main unit above the sedimentary cover structure. Conceptual problems of lithological studies in Russia: Materials of the 6th All-Russian lithological meeting, Kazan, 2011.
2. Butorin A. V. Study of the detailed structure of the Achimov oil and gas complex based on spectral decomposition of a seismic wave field - Text of the dissertation, St. Petersburg, 2016
3. M. V. Bukatov, D. N. Peskova, M. G. Nenasheva, S. A. Pogrebnuk, G. M. Timoshenko, D. V. Solodov, V. V. Zhukov, A. S. Bochkov, G. V. Volkov, A. A. Vashkevich. Key problems of Achimov deposits development on the different scales of studying (In Russ.), PRONEFT". *Professional'no o nefti*, 2018, no. **2** (8), pp. 16–21.
4. Nezhdanov A. A. Geological interpretation of seismic data: lecture course. TRU, Tyumen, 2017.
5. Nezhdanov A. A., Ponomarev V. A., Turenkov N. A., Gorbunov S. A. Geology and oil and gas potential of the Achimov sequence of Western Siberia. Publishing House of the Academy of Mining Sciences, Moscow, 2000.
6. Chakraborty, A., and Okaya, D.: Frequency-time decomposition of seismic data using wavelet-based methods, *Geophysics*, **60**, 1906–1916, 1995.
7. Chopra, S., and Marfurt, K.: Is curvature overrated? *No, it depends on the geology, First Break*, **33**, 45–55, 2015.
8. Chopra, S., and Marfurt, K.: Seismic attributes for prospect identification and reservoir Characterization, *SEG Geophysical Development Series* **11**, 327–35, 2007.
9. Chopra, Satinder & Marfurt, Kurt. (2005). Seismic attributes - A Historical Perspective. *Geophysics*. **70**. 3-. 10.1190/1.2098670
10. Continous Wavelet Transform, and S Transform. 6th International Conference and Exposition on Petroleum Geophysics, Kolkata, 662–666, 2006.
11. Harold Ryan.: Ricker, Ormsby, Klander, Butterworth - A Choice of Wavelets. - *CSEG Recorder*, Vol. **19**, Issue No. 07 (September 1994).

12. Laughlin, K., Garossino, P., and Partyka, G.: Spectral decomposition applied to 3D, *AAPG Explorer*. **23**, 28–31, 2002
13. Morlet, J., Arens, G., Fourgeau, E., and Glard, D.: Wave propagation and sampling theory-Part I: Complex signal and scattering in multilayered media, *Geophysics*, **47**, 203–221, 1982.
14. Partyka, G. A., Gridley, J., and Lopez, J.: Interpretational applications of spectral decomposition in reservoir characterization, *The Leading Edge*, **18**, 353–360, 1999.
15. Saadatinejad, M. R., Hassani, H., and Javaherian, A.: Representation of the thickness distribution of channels and stratigraphic events at one of the Iranian field in the Hormuz strait using a composite plot and RGB display technique, *Journal of Geophysics and Engineering*, **8**, 412–421, 2011, doi: 10.1088/1742-2132/8/3/002
16. Sinha, S., Routh, P. S., Anno, P. D., and Castagna, J. P.: Spectral decomposition of seismic data with continuous-wavelet transform, *Geophysics*, **70**,19–25, 2005.
17. Wawrzyniak, Kamila. (2009). Application of time-frequency transforms to processing of full waveforms from acoustic logs. *Acta Geophysica*. **58**. 49–82. 10.2478/s11600-009-0043-4.
18. Widess, M. B., 1973, How thin is a thin bed, *Geophysics*,**38**, 1176–1180
19. Zabibi, N. E., and Siahkoohi, H. R.: Single frequency seismic attribute based on Short Time Fourier Transform.